

User Guide for **Land Surface Atmospheric Boundary Interaction Product (LANDMET)**

William B. Rossow
Cindy Pearl

The City College of New York NOAA/CREST

Release Date: Nov 16 2016

Produced through the project “**GLOBALLY MERGED, RECONCILED AND
GRIDDED OBSERVATIONS OF NEAR-SURFACE ATMOSPHERIC AND LAND
SURFACE PROPERTIES AND THEIR DIURNAL-TO-DECADAL VARIATIONS**”
funded by NASA GRANT NO: NNX13AI22A

Table of Contents

| | |
|---|----|
| Summary:..... | 3 |
| 1. Sources of Data and Their Characteristics | 4 |
| 1.1 Ancillary Quantities | 4 |
| 1.2. Daily Quantities | 5 |
| Constant quantities (reported for convenience): | 5 |
| Variable quantities: | 5 |
| 1.3. 3-Hourly Quantities..... | 6 |
| 2. Reconciliations | 7 |
| 3. Space-Time Variability & Filling Procedures | 8 |
| 4. Converting equal-area map to equal-angle map | 10 |
| 5. References..... | 10 |
| 6. Appendix – Known Errors | 14 |
| 7. Appendix – NC_DUMP..... | 14 |
| 8. Appendix – Sample Images for Each Variable from 2003 01 01 | 28 |

Summary:

Investigations of land-atmosphere interactions have usually tended to rely, in part, on a variety of models to describe either atmospheric conditions near the land surface (global or regional weather analyses or forecast models) or the variations of land surface properties forced by changing weather conditions (land surface models) because some aspects of the near-surface meteorology or land properties were not readily available from observations. In fact there is a rich variety of observations available from conventional surface-based and satellite sources, but these have generally been used in “piecemeal” comparisons to these models, not usually as an integrated set of information that encompasses the whole complex of land-atmosphere interactions. Earlier projects to pull together global, combined data products, namely the International Satellite Land Surface Climatology Project (ISLSCP I and II, Hall *et al.* 2006) and the Global Soil Wetness Project (GSWP, which used some of the ISLSCP product, Dirmeyer *et al.* 1999), were focused primarily on assembling a comprehensive set of the atmospheric “forcing” for land surface models (LSMs).

This new product is a multi-variate data compilation that reconciles the variation scales of these multiple measurements, merges and maps them into a comprehensive description of the near-surface atmospheric properties together with the land surface property variations on diurnal-to-decadal time scales. The land surface is represented by land fraction, land surface type, topography (mean and standard deviation), total effective and black sky spectral albedoes at solar wavelengths, thermal effective infrared and microwave emissivities, temporary flooding fraction, soil moisture, snow cover fraction and skin temperature. The atmosphere is represented by temperature and humidity profiles from the surface up to the 500 hPa level, surface windspeed, precipitation amount and type, low-level cloud types and amounts, net SW and LW radiative fluxes at the surface and at 680 hPa, and turbulent sensible and latent heat fluxes at the surface. Despite the increase of the number of available data products, their differences in space-time resolution preclude making a merged product at finer spatial intervals than about 100 km and finer time intervals than daily, but any product with finer time sampling is reported here at 3-hr intervals. The time period overlap among the products covers only 10 years, 1998-2007. In other words, available data still do not allow for much improvement over the first ISLSCP product in terms of space-time resolution and coverage. The LANDMET data product is comprised of a sequence of daily global files, where quantities are mapped into 1.0-degree-equivalent equal-area grid. The format is netCDF-4.

Many of these data products, especially those based on surface measurements, are spatially and/or temporally sparse or incomplete in coverage, so procedures were developed to fill missing values. These procedures are based on evaluations of the characteristic space-time scales of variability of each quantity. Because of the spatial heterogeneity of the land surface and larger-scale variations of the atmosphere, time interpolation at each location is the preferred filling method.

The LANDMET product is comprised of 4 Ancillary products that are fixed in time but vary with location, 3 Land Surface properties that vary at daily intervals and 7 Surface and Lower Atmospheric properties that vary at 3-hr intervals. The global maps are arranged in daily files with eight components for those quantities reported at 3-hr intervals.

1. Sources of Data and Their Characteristics

1.1 Ancillary Quantities

Land Surface Type: The land surface type information includes, for each map grid cell, the type and coverage fractions of the top three surface types present in the cell. The sum of these three fractions may not equal the land fraction if more types are present (usually a small difference). This information is taken from the ISCCP SURFACETYPE product (ISCCP C-ATBD), which is a merger of the IGBP-DISC surface type product (Loveland *et al.* 2009, obtained from the USGS EROS data center at http://daac.ornl.gov/ISLSCP_II/guides/edc_landcover_xdeg.html) and the GLIMS permanent glacier cover product (Armstrong *et al.* 2005, obtained from <http://www.glims.org>), both of which have been reconciled to the ISCCP TOPO land fraction (see below). The ISCCP SURFACETYPE product has an original equal-area mapping at 0.25 degrees-equivalent, but is here reduced to 1.0 degree equal-area.

Total Effective and Spectral Albedos: The Total Effective Surface Albedo at solar wavelengths is taken from the ISCCP FD radiative fluxes product (2.5 degree-equivalent equal-area, Zhang *et al.* 2004) and the Spectral Albedos are from the MODIS black-sky product (1 km interval,

https://www.umb.edu/spectralmass/terra_aqua_modis/modis_brdf_albedo_cmg_gap_filled_snow_free_product_mcd43gf_v005, Moody *et al.* 2005) at seven wavelengths (0.47, 0.55, 0.67, 0.86, 1.24, 1.64 and 2.1 μm). The albedo estimates used in the ISCCP FD flux calculations were determined from the retrieval of visible reflectance and a surface-type-dependent spectral representation that was compared with the MODIS product; the largest differences occurred at wavelengths longer than about 0.8 microns but had little effect on the calculated net SW flux at the surface. The value reported as the Total Effective Albedo is determined from the ratio of the upwelling to downwelling SW fluxes in the ISCCP FD product, representing an average over all wavelengths and all-sky illumination conditions. The monthly mean and standard deviation were calculated for MODIS from the original 5 km resolution. The monthly mean FD values were extracted from the 2.5 degree equal-area product and saved at 1.0 degree equal-area.

Thermal Effective Infrared and Microwave Emissivities: The broadband thermal IR emissivity is taken from the ISCCP FD radiative fluxes product (2.5 degree equal-area, Zhang *et al.* 2004), the emissivity at 10.5 microns is from the ISCCP IREMISS product (0.25 degree equal-area, ISCCP C-ATBD) and the microwave emissivities at four frequencies and two polarizations is from the combined analysis of SSM/I and window IR based on ISCCP DX product (0.25 degree equal-area, Aires *et al.* 2001). The broadband thermal infrared emissivity is the ratio of the upwelling LW flux to the blackbody flux at the given surface skin temperature. The IREMISS values are produced by a reconciliation of three products from AIRS (V6 L2, Chahine *et al.* 2006, http://disc.sci.gsfc.nasa.gov/AIRS/documentation/v6_docs), MODIS (Wan 2014) and IIR (*e.g.*, Garnier *et al.* 2012). The monthly mean broadband thermal emissivity from FD was extracted from the 2.5 degree product and saved at 1.0 degree equal-area. The surface microwave emissivity was extracted at 0.25 degrees and the monthly mean and standard deviation saved at 1.0 degree equal-area. The ISCCP IREMISS was weighted by the percentage

of each type found in each equal cell of the ISCCP SURFACETYPE product, and the resulting emissivities were saved at 1.0 degree equal-area.

1.2. Daily Quantities

Constant quantities (reported for convenience):

Land Fraction: The fraction of land in each grid cell is taken from the ISCCP TOPO data product (ISCCP C-ATBD), which combines and reconciles the GTOPO30 product and the 1 KM AVHRR land mask product from the USGS EROS data center (respectively, <http://lta.cr.usgs.gov/GTOPO30>, http://edc2.usgs.gov/1KM/land_sea_mask.php). The permanent open water fraction is given by 1.0 minus the land fraction.

Topography: The mean and standard deviation of topographic height (in meters) is taken from the ISCCP TOPO product, which is a reconciliation of the GTOPO30 (original grid interval about 0.9 km, obtained from the USGS EROS data center at <http://lta.cr.usgs.gov/GTOPO30>) and the AVHRR 1KM Land Mask (obtained from the USGS EROS data center at http://edc2.usgs.gov/1KM/land_sea_mask.php). Comparison of these two products led to small adjustments of land fraction, favoring GTOPO30 at the coastlines, but retaining the AVHRR 1KM identification of larger inland lakes. These two products were also compared to the ETOPO product; differences were “noise-like” but concentrated at coastlines and in high topography regions. These quantities were mapped to a 0.1 degree-equivalent equal-area map (about 10 km intervals) and then reduced to 1.0 degree-equivalent equal-area. These quantities are supplied daily for ease of use.

Variable quantities:

Temporary Flooding Fraction: The flooding fraction, interpreted as the additional coverage by open water beyond the permanent fractional coverage (1.0 – land fraction), is taken from the monthly Inundation product (noaaacrest.org/rscg/Produts/LSH/extent.html, Papa *et al.* 2006, 2007, 2008a, 2008b, Prigent *et al.* 2007), which is mapped at 0.25 degree equal-area. This product was compared in specific regions to a much higher resolution satellite radar product. The all-record minimum inundation fraction was compared to the permanent open water fraction (1.0 – land fraction) and found to be in general agreement to within about 5%; slightly larger positive differences were concentrated in the Canadian lakes region. Therefore the Inundation product was converted to an anomaly fraction by subtracting the all-record minimum value at each location. These monthly anomalies were re-mapped to 1.0 degree equal-area and linearly interpolated between mid-month dates to produce values for each day.

Soil Moisture: The soil moisture (in m^3/m^3) information comes from the GEWEX fusion of satellite active and passive microwave measurements (<http://www.esa-soilmoisture-cci.org>; contact = cci_sm_contact@eodc.eu, Liu, *et al.* 2011, 2012, Wagner *et al.* 2012) at daily intervals in a 0.25 degree equal-angle map grid. The soil porosity and wetlands coverage from this product are also reported as Ancillary information. These quantities are re-mapped to a 1.0 degree equal-area grid.

Snow Cover Fraction: The daily snow cover fraction at 0.25 degree equal-area is from the

Microwave Snow product (noaaacrest.org/rscg/Produts/LSH/snowcover.html, Shahroudi and Rossow 2014) for 1998 -2004 and the 0.25 degree resolution ISCCP SNOWICE product for 2005-2007. The first is derived from an analysis of the SSM/I-DX microwave emissivities. This product was evaluated against three other snow products, including the one produced from MODIS (Shahroudi and Rossow 2014). The second is based on the NOAA NSIDC IMS Daily Northern Hemisphere Snow and Ice Analysis at 24 km Resolution (Helfrich *et al.* 2012). The snow cover fractions are averaged into a 1.0 degree equal-area.

1.3. 3-Hourly Quantities

Skin Temperature: The skin temperature (in Kelvins) is taken from the ISCCP FD product (2.5 degree equal-area grid) (Zhang *et al.* 2004, 2007). This product was evaluated by comparisons to results from MODIS and AIRS. The skin temperatures are extracted from the original 2.5 degree equal-area grid and mapped into a 1.0 degree equal-area grid.

Atmospheric Temperature-Relative Humidity Profile: The atmospheric profiles of temperature (in Kelvins) and relative humidity (in percent) from the surface to the 500 hPa level are taken from the ISCCP NNHIRS product (1.0 degree equal-area grid, ISCCP C-ATBD) that is based on a new analysis of HIRS IR sounder measurements (Shi *et al.* 2016). This product was evaluated against the ARSA collection of radiosondes (Analyzed RadioSounding Archive (ARSA) database, <http://ara.abct.lmd.polytechnique.fr/index.php?page=arsa>) and surface weather station reports (ISD, see next).

Surface Windspeed: The surface windspeeds (in m/s) are from the ISD collection of surface weather station reports (www.ncdc.noaa.gov/isd, Smith *et al.* 2011). These estimates are reported on a 1.0 degree-equivalent equal-area grid; the number of stations averaged is also given. The values of near-surface air temperature and relative humidity from the surface measurements are also reported.

Precipitation Rate, Type and Fraction: The precipitation rate (in mm/hr) is a merger of the TMPA product (mapped at 0.25 degrees) for latitudes equatorward of 50 degrees (Huffman *et al.* 2007) and the GPCP product (mapped at 1.0 degrees) for the polar regions (<http://precip.gsfc.nasa.gov/> -- for info: http://precip.gsfc.nasa.gov/gpcp_daily_comb.html, Huffman *et al.* 2001). The daily GPCP values are divided equally among eight times of day, converting mm/day to mm/hr (*cf.* Rossow *et al.* 2013). These two products were compared to each other for consistency; the GPCP product over land merges satellite and surface-based measurements. Precipitation type is determined by the corresponding near-surface air temperature (TA) from the ISCCP NNHIRS product: flag = 0 is liquid precipitation and flag = 1 is frozen precipitation when TA < 268 K. Any location flagged as undefined in the TMPA product is filled with values from GPCP; an Origin Code is included (0 for TMPA, 1 for GPCP). The precipitation fraction, defined as the ratio of the average precipitation including and excluding zero values, is reported to indicate area extent of precipitation. These quantities were re-mapped from a 1.0 degree equal-angle grid to a 1.0 degree equal-area grid.

Low-level Cloud Properties: The low-level cloud types and cover fractions, along with the total and deep convective cloud fraction, are reported together with the lowermost cloud base pressure, uppermost cloud top pressure and total cloud fraction. These quantities are taken from the ISCCP FD radiative flux product (mapped on a 2.5 degree equal-area grid), which is a combination of the ISCCP D-Version cloud products (Rossow and Schiffer 1999) and a statistical model used to estimate the cloud properties for layers not seen directly from the

satellite (Zhang *et al.* 2004). The statistical model has been evaluated by comparison to the merged CloudSat-Calipso cloud vertical profiles (Rossow and Zhang 2010). A low-level cloud is reported if uppermost cloud top pressure for the lowest cloud layer present is greater than 500 hPa, but deep convective cloud fraction is included regardless of top pressure. The presence of other cloud layers is indicated by a difference between total and low-cloud amounts. These quantities are re-mapped to 1.0 degree equal-area.

Net SW and LW Radiative Fluxes: The net SW and LW fluxes (in W/m^2) at the surface and at the 680 hPa level are taken from the ISCCP FD radiative fluxes product (2.5 degree equal-area grid, Zhang *et al.* 2004). The sign of the net fluxes indicates energy **into** the atmospheric layer from 680 hPa to the surface. For example, the net SW (LW) flux at 680 hPa is positive (negative) and negative (positive) at the ground. The surface radiative fluxes have been evaluated against other similar products from GEWEX SRB and CERES and against the BSRN reference network. The near-surface air temperature used to calculate downwelling LW fluxes is also reported. These quantities are re-mapped to 1.0 degree equal-area.

Sensible and Latent Heat Fluxes: These fluxes (in W/m^2) come from the Princeton product that is a prototype of the GEWEX LANDFLUX products. The input data is mapped at 0.5 degree square-grid and is obtained from <http://hydrology.princeton.edu/data/landflux/>, Vinukollu *et al.* 20011). Quantities included are contributions to total evapotranspiration from plant transpiration, wet canopy, soil, snow and open water. These quantities are re-mapped to 1.0 degree equal-area.

2. Reconciliations

The land fraction, land surface type and topography datasets from different sources are reconciled in terms of their land fractions, taking the much higher resolution topography and AVHRR 1KM land masks as the references. The latter two products are adjusted so as to preserve the identification of large inland lakes in the AVHRR 1KM product – the topography dataset reports heights for these locations, which are retained, without discriminating the surface type (ISCCP C-ATBD). This version of these datasets reports consistent land fractions at 0.25 degree equal-area, which are then averaged to 1.0 degree equal-area.

The ISCCP FD radiative flux product assumes that the spectral dependence of surface albedo is determined by surface types but consistent with the ISCCP Cloud Product visible reflectances for each location (Zhang *et al.* 2004). The spectral shape of the surface albedo as a function of surface type was compared with the MODIS spectral albedo product (black sky). The FD spectral shapes were biased relative to the MODIS product, but entirely in the near-IR at wavelengths longer than about 0.8 microns. Using the MODIS products in the calculations did not change the net SW fluxes by more than a few percent. Hence the MODIS product reported here is consistent with the FD net SW surface fluxes. The total surface albedo reported here is the ratio of upwelling to downwelling SW fluxes from the ISCCP FD product, equivalent to an illumination spectrum-weighted value for all sky conditions (clear and cloudy sky) and the MODIS spectral albedos are the black sky version.

The thermal infrared emissivity at 10.5 μm wavelength from IREMISS is based on the reconciliation of three products sorted by surface type, from the MODIS LST product, the AIRS LST product and another LST product from the IIR instrument on the Calipso satellite. These

products are compared for overlapping years, showing little time-variability. Generally the results agree to better than one percent; the few cases of disagreement are resolved in favor of the MODIS results.

The 16-yr minimum flooding fraction from the monthly inundation product at each location was compared to permanent water fraction ($1.0 - \text{land fraction}$) in the reconciled surface type dataset. In general the minimum fraction agreed to within 5% fractional area at 0.25 degree equal-area; the few regions with somewhat larger disagreements were concentrated in the central Canadian lake region. Therefore, the reconciliation of these two water fraction datasets was done by converting the inundation values into time-record-anomalies by subtracting the record-minimum at each location. This anomaly value is then linearly interpolated from monthly (assigned to the mid-month day) to daily values and interpreted as the additional water fraction over and above the permanent water fraction.

The Soil Moisture is compared to the temporary flooding and precipitation products for consistency. The near-surface air temperature from ISCCP NNHIRS is used to remove values reported for locations that are too cold to have liquid water present near the surface; soil moisture values for any locations that are labeled as permanent glacier in the surface type product are also removed.

As part of the snow cover fraction retrieval from combined microwave and infrared satellite measurements, the presence of snow is required to be consistent with surface skin temperatures below 273 K.

Over land the ISCCP NNHIRS temperature and humidity profiles were compared to ARSA radiosondes, showing that there were no significant biases in temperature or humidity. However, the comparison of near-surface air temperatures and humidities to the ISD surface weather station reports showed a small (of order a few degrees) temperature-dependent bias in temperatures. The near-surface air temperatures were corrected to reduce these biases. Although the comparison suggests that the NNHIRS near-surface humidities are slightly smaller than the ISD values, the magnitude of this bias is generally within the uncertainties, so no change was made. The ISD values of near-surface temperature and relative humidity are also reported for comparison.

The two precipitation products, TMPA (3-hourly) and GPCP (daily), are produced from similar satellite inputs and merged with surface gauge data over land. The former product uses a more modern microwave retrieval and measurements from all available microwave instruments to obtain 3-hr sampling, whereas the latter uses data from only one microwave instrument at a time to obtain daily sampling. The former does not report values poleward of 50° but the latter uses satellite infrared measurements to fill in at higher latitudes. The agreement of the daily precipitation values from these two datasets is generally good, so we use TMPA as the main dataset but its coverage is completed using GPCP. The GPCP daily precipitation in mm/day is converted to mm/hr by dividing the daily amount equally among eight times per day (*cf.* Rossow *et al.* 2013).

3. Space-Time Variability & Filling Procedures

The daily soil moisture maps have many gaps. The first step to fill these is to linearly interpolate in time over a time interval up to ± 15 days at each location that is missing values. If only one valid value is available, then that value is replicated. If both available values (previous and subsequent) are labeled as “too cold”, the missing value is also labeled as too cold. If the

time interpolation fails, the missing values are filled from a 12-monthly climatology produced solely from the original data but filled by linear interpolation over longitude at each latitude. Even after these two steps, there are regions in the tropics that are still missing – presumably due to the interference of persistent cloud cover and precipitation with satellite microwave measurements; thus, the soil moisture at these locations is filled with the record-maximum value ($0.66 \text{ m}^3/\text{m}^3$).

Because of cloud effects on the measurements and the usual situation of measurements obtained from two instruments on satellites in sun-synchronous orbits, infrared temperature-humidity sounding products generally provide about 10-30% coverage of the globe at four times of day. To achieve the goal of adequate diurnal resolution and to compensate for the inhomogeneous time-of-day sampling over the whole time record, the NNHIRS product uses a statistical model of the diurnal variations of temperature, based on an 8-yr period (02/2001-01/2009) with three-to-four satellite coverage (six to eight samples per day). The statistical model was developed by, first, fitting the monthly mean diurnal anomalies (deviations from the average over all times of day for each satellite separately) at local hour intervals at each pressure level with a cubic spline. Then PCA is performed on the hourly anomalies from the daily mean temperature for each grid cell at each pressure level over the whole period 02/2001-01/2009. The final diurnal variation model uses only the first three PCs to smooth out the variations, which explains about 94% over land (*cf.* Aires *et al.* 2004). The rms differences between the 3-term and the all-term PCA representations were found to increase as the diurnal amplitude decreases so the PCA model was restricted to locations where the diurnal range is $\geq 2 \text{ K}$: over all land areas at pressure levels $\geq 500 \text{ hPa}$. Daily mean T profiles are determined for all days that have at least one daytime and one nighttime sample; the PCA-based bias corrections are applied to correct for the specific time-of-day sample available. If a daily mean value is not available on a particular day, the daily mean is obtained by interpolating from nearby daily mean values in a ± 5 -day interval. If the interpolation fails because data are not available, the monthly averaged daily mean value is used; if there is no monthly mean, then the climatology for the appropriate month is used. The PCA model of diurnal anomalies is then applied to the daily mean T profiles from the surface up to the 500 hPa level. Based on ISD, the diurnal variations of humidity are small, the NNHIRS values the daily minimum values. Missing daily values are filled by linear interpolation of daily minimum (mean) values over a ± 5 -day interval. If this interpolation fails, the monthly mean daily minimum value is used; if the monthly mean value is missing, the climatology from 02/2001-01/2009 is used.

The surface windspeed data generally have good time resolution and coverage but are completely absent in some regions. To fill in missing data, the first step was to create maps at each time step at different spatial resolutions, 1.0, 2.5 and 5.0 degree-equivalent equal-area, where all available values are averaged. Some map grids at each resolution contain values from a single station. Some missing values in all maps are then filled by linear interpolation in time up to an interval of ± 2 days; if only one value is available, it is replicated. Some additional missing values in the 5.0 degree map are filled by linear interpolation over longitude at each latitude. The remaining missing values in the 1.0 degree map are then filled by values from the 2.5 degree map; if no values are available from the 2.5 degree map, the fill values are taken from the 5.0 degree map.

4. Converting equal-area map to equal-angle map

All of the quantities in this dataset are stored in a 1-degree-equivalent equal-area map; This mapping maintains approximately equal-areas by varying the longitude interval at each latitude; the latitude intervals are constant at 1 degree. Appendix 7 provides a simple procedure that uses map grid information in the dataset to re-project the data into a 1-degree equal-angle form. Following the pseudo code are sample maps and histograms for variables found in the 2003 01 01 netcdf file. The pseudo code is also included here for your convenience. By applying the following pseudo code an equal-area grid image can be represented as an equal-angle grid.

Retrieve variables from the netcdf file (In this example the physical variable is ttrop):

```
sqlon_beg,  
sqlon_end,  
eqlat_index  
eqcell  
ttrop  
  
do icell=1,eqcell  
  ilon1 = sqlon_beg(icell)  
  ilon2 = sqlon_end(icell)  
  ilat = eqlat_index(icell)  
  do i=ilon1,ilon2  
    sqmap(i,ilat) = ttrop(icell)  
  enddo  
enddo
```

The variable `sqmap(360,180)` can now be displayed in equal angle format.

5. References

- Aires, F., C. Prigent, W.B. Rossow and M. Rothstein, 2001: A new neural network approach including first-guess for retrieval of atmospheric water vapor, cloud liquid water path, surface temperature and emissivities over land from satellite microwave observations. *J. Geophys. Res.*, **106**, 14,887-14,907.
- Aires, F., C. Prigent and W.B. Rossow, 2004: Temporal interpolation of global surface skin temperature diurnal cycle over land under clear and cloudy conditions. *J. Geophys. Res.*, **109**, doi 10.1029/2003JD003527 (1-18).
- Armstrong, R., B. Raup, S.J.S. Khalsa, R. Barry, J. Kargel, C. Helm and H. Kieffer, 2005: *GLIMS glacier database*, Boulder, CO: National Snow and Ice Data Center Digital media: <http://nsidc.org/data/nsidc-0272.html>.
- Chahine, M.T., T.S. Pagano, H.H. Aumann, R. Atlas, C. Barnet, J. Blaisdell, L. Chen, M. Divakarla, E.J. Fetzer, M. Goldberg, C. Gautier, S. Granger, S. Hannon, F.W.

- Irion, M. Kakar, E. Kalnay, B.H. Lambrigsten, S-Y. Lee, J. Le Marshall, W.W. McMillan, L. McMillin, E.T. Olsen, H. Revercomb, P. Rosenkranz, W.L. Smith, D. Staelin, L. Larrabee Strow, J. Susskind, S. Tobin, W. Wolf and L. Zhou, 2006: AIRS: Improving weather forecasting and providing new data on greenhouse gases. *Bull. Amer. Meteor. Soc.*, **87**, 911-926, doi:10.1175/bams-87-7-911.
- Dirmeyer, P.A., A.J. Dolman and N. Sato, 1999: The pilot phase of the global soil wetness project. *Bull. Amer. Meteor. Soc.*, **80**, 851-878.
- Garnier, A., J. Pelon, P. Dubuisson, M. Faivre, O. Chomette, N. Pascal and D.P. Kratz, 2012: Retrieval of cloud properties using CALIPSO Imaging Infrared Radiometer, Part I: Effective emissivity and optical depth. *J. Appl. Meteor. Climate*, **55**, doi:10.1175/JAMC-D-11-0220.1.
- Hall, F.G., E. Brown de Colstoun, G.J. Collatz, D. Landis, P. Dirmeyer, A. Betts, G.J. Huffman, L. Bounoua and B. Meeson, 2006: ISLSCP Initiative II global data sets: Surface boundary conditions and atmospheric forcings for land-atmosphere studies. *J. Geophys. Res.*, **111**, doi:10.1029/2006JD007366.
- Helfrich, S.R., M. Li and C. Kongol, 2012: Interactive Multisensor Snow and Ice Mapping System Version 3 (IMS V3) algorithm theoretical basis document version 2.1. NOAA NESDIS Center for Satellite Applications and Research (STAR), 61pp.
- Huffman, G.J., R.F. Adler, M. Morrissey, D.T. Bolvin, S. Curtis, R. Joyce, B. McGavock and J. Susskind, 2001: Global precipitation at one degree daily resolution from multisatellite observations. *J. Hydrometeor.*, **2**, 36-50.
- Huffman, G.J., D.T. Bolvin, E.J. Nelkin, D.B. Wolff, R.F. Adler, G. Gu, Y. Hong, K.P. Bowman and E.F. Stocker, 2007: The TRMM multisatellite precipitation analysis (TMPA): Quasi-global, multi-year, combined-sensor precipitation estimates at fine scales. *J. Hydrometeor.*, **8**, 38-55.
- ISCCP H-Version Climate Algorithm Theoretical Basis Document, NOAA Climate Data Record Program at <http://www.ncdc.noaa.gov/cdr/operationalcdrs.html>.
- Liu, Y.Y., Dorigo, W.A., Parinussa, R.M., de Jeu, R.A.M., Wagner, W., McCabe, M.F., Evans, J.P., van Dijk, A.I.J.M. (2012). Trend-preserving blending of passive and active microwave soil moisture retrievals, *Remote Sensing of Environment*, 123, 280-297, doi: 10.1016/j.rse.2012.03.014.
- Liu, Y.Y., Parinussa, R.M., Dorigo, W.A., De Jeu, R.A.M., Wagner, W., van Dijk, A.I.J.M., McCabe, M.F., & Evans, J.P. (2011): Developing an improved soil moisture dataset by blending passive and active microwave satellite based retrievals. *Hydrology and Earth System Sciences*, 15, 425-436.
- Loveland, T., J. Brown, D. Ohlen, B. Reed, Z. Zhu, L. Yang and S. Howard, 2009: ISLSCP II IGBP DISCover and SiB land cover, 1992-1993, In F.G. Hall, G. Collatz, B. Meeson, S. Los, E. Brown de Colstoun and D. Landis (Eds.) *ISLSCP Initiative II Collection Data Set*, (available on line from Oak Ridge National Laboratory Distributed Active Archive Center, Oak Ridge, TN, doi:10.3334/ORNLDAAAC/930.

- Moody, E.G., M.D. King, S. Platnick, C.B. Schaaf and F. Gao, 2006: Spatially complete global spectral surface albedos: Value-added datasets derived from TERRA MODIS land products. *IEEE*, **43**, doi:10.1109/TGRS.2004.838359.
- Papa, F., C. Prigent, F. Durand and W.B. Rossow, 2006: Wetland dynamics using a suite of satellite observations: A case study of application and evaluation for the Indian subcontinent. *Geophys. Res. Lett.*, **33**, doi: 10.1029/2006GL025767, (1-4).
- Papa, F., C. Prigent and W.B. Rossow, 2007: Ob' river inundations from satellite observations: A relationship with winter snow parameters and river runoff. *J. Geophys. Res.*, **112**, D18103, doi 10.1029/2007JD008451, (1-11).
- Papa, F., A. Guntner, F. Frappart, C. Prigent and W.B. Rossow, 2008a: Variations of surface water extent and water storage in large river basins: A comparison of different global data sources, *Geophys. Res. Lett.*, **35**, L11401, doi: 10.1029/2008GL033857 (1-5).
- Papa, F., C. Prigent and W.B. Rossow, 2008b: Monitoring flood and discharge variations in the large Siberian rivers from a multi-satellite technique. *Surv. Geophys.*, doi: 10.1007/s10712-008-9036-0, (1-21).
- Prigent, C., F. Papa, F. Aires, W.B. Rossow and E. Matthews, 2007: Global inundation dynamics inferred from multiple satellite observations, 1993-2000. *J. Geophys. Res.*, **112**, D12107, doi: 1029/2006JD007847, (1-13).
- Rossow, W.B., and R.A. Schiffer, 1999: Advances in understanding clouds from ISCCP. *Bull. Amer. Meteor. Soc.*, **80**, 2261-2287.
- Rossow, W.B. and Y-C. Zhang, 2010: Evaluation of a statistical model of cloud vertical structure using combined CloudSat and Calipso cloud layer profiles. *J. Climate*, **23**, 6641-6653.
- Rossow, W.B., A. Mekonnen, C. Pearl and W. Goncalves, 2013: Tropical precipitation extremes. *J. Climate*, **26**, 1457-1466, doi: 10.1175/JCLI-D-11-00725.1.
- Shahroudi, N., and W.B. Rossow, 2014: Using microwave surface emissivities to isolate the signature of snow on different land surface types. *Remote Sensing Environ.*, **152**, doi:10.1016/j.rse.2014.07.008, 638-653.
- Shi, L., J.L. Matthews, S-P. Ho, Q. Yang and J.J. Bates, 2016: Algorithm development of temperature and humidity profile retrievals for long-term HIRS observations. *Remote Sens.*, **8**, 280, (1-17), doi:10.3390/rs8040280.
- Smith, A., N. Lott and R. Vose, 2011: The Integrated Surface Database: Recent developments and partnerships. *Bull. Amer. Meteor. Soc.*, **92**, 704-708, doi:10.1175/2011BAMS3015.1.
- Vinukollu, R.K., E.F. Wood, C.R. Ferguson and J.B. Fisher, 2011: Global estimates of evapotranspiration for climate studies using multi-sensor remote sensing data: Evaluation of three process-based approaches. *Remote Sens. Environ.*, **115**, 801-823, doi:10.1016/j.rse.2010.11.006.
- Wagner, W., W. Dorigo, R. de Jeu, D. Fernandez, J. Benveniste, E. Haas, M. Ertl (2012): Fusion of active and passive microwave observations to create an Essential Climate Variable data record on soil moisture. ISPRS Annals of the Photogrammetry, Remote Sensing and Spatial Information Sciences, Volume I-7, 2012. XXII ISPRS Congress, 25 August – 01 September 2012, Melbourne, Australia.
- Wan, Z., 2014: New refinements and validation of the collection-6 MODIS land-surface temperature/emissivity product. *Remote Sens. Environment*, **140**, 36-45.

- Zhang, Y-C., W.B. Rossow, A.A. Lacis, M.I. Mishchenko and V. Oinas, 2004: Calculation of radiative fluxes from the surface to top-of-atmosphere based on ISCCP and other global datasets: Refinements of the radiative transfer model and the input data. *J. Geophys. Res.*, **109**, doi 10.1029/2003JD004457 (1-27 + 1-25).
- Zhang, Y., W. B. Rossow, and P. W. Stackhouse, 2006: Comparison of different global information sources used in surface radiative flux calculation: Radiative properties of the near-surface atmosphere. *J. Geophys. Res.*, **111**, D13106, doi: 10.1029/2005JD006873, (1-13).
- Zhang, Y-C., W.B. Rossow and P.W. Stackhouse, 2007: Comparison of different global information sources used in surface radiative flux calculation: Radiative properties of the surface. *J. Geophys. Res.*, **112**, D01102, doi: 10.1029/2005JD007008, (1-20).

6. Appendix – Known Errors

variables pmaxt and ptrop in file landmet_L3_<date>_v1: should be listed as units= hPa

7. Appendix – NC_DUMP

```
netcdf landmet_L3_20030101_v1 {
dimensions:
    edge = 2 ;
    label_len = 22 ;
    eqcell = 41252 ;
    eqzone = 180 ;
    lon = 360 ;
    lat = 180 ;
    levels_t = 7 ;
    levels_rh = 7 ;
    low_cloud_type = 12 ;
    times = 8 ;
variables:
    float eqlon(eqcell) ;
        eqlon:long_name = "Center longitude of equal-area cell" ;
        eqlon:units = "degrees_east" ;
        eqlon:valid_min = 0. ;
        eqlon:valid_max = 360. ;
    float eqlat(eqcell) ;
        eqlat:long_name = "Center latitude of equal-area cell" ;
        eqlat:units = "degrees_north" ;
        eqlat:valid_min = -90. ;
        eqlat:valid_max = 90. ;
    short eqlon_index(eqcell) ;
        eqlon_index:long_name = "Longitude index of equal-area cell" ;
        eqlon_index:units = "1" ;
        eqlon_index:valid_min = 1 ;
        eqlon_index:valid_max = 360 ;
    short eqlat_index(eqcell) ;
        eqlat_index:long_name = "Latitude index of equal-area cell" ;
        eqlat_index:units = "1" ;
        eqlat_index:valid_min = 1 ;
        eqlat_index:valid_max = 180 ;
    short eqcells_in_zone(eqzone) ;
        eqcells_in_zone:long_name = "Number of longitude cells in each
equal-area zone" ;
        eqcells_in_zone:units = "1" ;
        eqcells_in_zone:valid_min = 1 ;
        eqcells_in_zone:valid_max = 360 ;
    int eqarea(eqcell) ;
        eqarea:long_name = "Equal-area cell area" ;
        eqarea:units = "km2" ;
    float lon(lon) ;
        lon:long_name = "Longitude" ;
```

```

        lon:units = "degrees_east" ;
        lon:valid_min = 0. ;
        lon:valid_max = 360. ;
        lon:bounds = "lon_bounds" ;
        lon:description = "Center longitude of square grid cell" ;
        float lon_bounds(lon, edge) ;
        lon_bounds:long_name = "Beginning and ending longitude for each
longitude zone" ;
        lon_bounds:units = "degrees_east" ;
        float lat(lat) ;
        lat:long_name = "Latitude" ;
        lat:units = "degrees_north" ;
        lat:valid_min = -90. ;
        lat:valid_max = 90. ;
        lat:bounds = "lat_bounds" ;
        lat:description = "Center latitude of square grid cell" ;
        float lat_bounds(lat, edge) ;
        lat_bounds:long_name = "Beginning and ending latitude for each
latitude zone" ;
        lat_bounds:units = "degrees_north" ;
        short sqlon_beg(eqcell) ;
        sqlon_beg:long_name = "Square grid beginning longitude index"
;
        sqlon_beg:units = "1" ;
        short sqlon_end(eqcell) ;
        sqlon_end:long_name = "Square grid ending longitude index" ;
        sqlon_end:units = "1" ;
        short utctime(times) ;
        utctime:long_name = "Time steps" ;
        utctime:units = "hour" ;
        utctime:valid_min = 0 ;
        utctime:valid_max = 21 ;
        utctime:description = "8 UTC/day every 3 hours since 00:00:00z
current day" ;
        short land_fraction(eqcell) ;
        land_fraction:long_name = "Land area fraction" ;
        land_fraction:units = "1" ;
        land_fraction:valid_min = 1 ;
        land_fraction:valid_max = 0 ;
        land_fraction:scale = 0.01 ;
        land_fraction:_FillValue = -9999s ;
        land_fraction:description = "Fraction of land found in equal
area cell" ;
        land_fraction:reference =
"http://www.noacrest.org/rscg/Products/SCT/topo.html" ;
        short height(eqcell) ;
        height:long_name = "Mean topographical height" ;
        height:units = "m" ;
        height:valid_min = 5417 ;
        height:valid_max = -48 ;
        height:description = "Mean topographical height above sea
level taken from ISCCP" ;

```

```

        height:reference =
"http://www.noacrest.org/rscg/Products/SCT/topo.html" ;
        short sigma_height(eqcell) ;
        sigma_height:long_name = "Topographic height standard
deviation" ;
        sigma_height:units = "m" ;
        sigma_height:valid_min = 1744 ;
        sigma_height:valid_max = 0 ;
        sigma_height:description = "Standard deviation of mean
topographical height taken from ISCCP " ;
        sigma_height:reference =
"http://www.noacrest.org/rscg/Products/SCT/topo.html" ;
        short floodfrac(eqcell) ;
        floodfrac:long_name = "Temporary flood area fraction " ;
        floodfrac:units = "1" ;
        floodfrac:valid_min = 0 ;
        floodfrac:valid_max = 1 ;
        floodfrac:scale = 0.01 ;
        floodfrac:_FillValue = -9999s ;
        floodfrac:description = "The fraction of the equal area cell
occupied by flooded land" ;
        floodfrac:reference =
"http://www.noacrest.org/rscg/Products/LSH/extent.html,Papa, F., C.
Prigent, and W.B. Rossow (2008): Monitoring flood and discharge variations
in the large Siberian rivers From a multi-satellite technique.Surv.
Geophys, doi:10.1007/s10712-008-9036-0,Papa, F., C. Prigent, F. Durand,
and W.B. Rossow (2006), Wetland dynamics using a suite of satellite
observations: A case study of application and evaluation for the Indian
Subcontinent,Geophys. Res. Lett.,33, L08401, doi:10.1029/2006GL025767" ;
        short vsm(eqcell) ;
        vsm:long_name = "Volumetric soil moisture where persistently
frozen values are removed." ;
        vsm:units = "m3 m-3" ;
        vsm:scale_factor = 0.001f ;
        vsm:valid_min = 0.f ;
        vsm:valid_max = 1.f ;
        vsm:_FillValue = -9999s ;
        vsm:description = "Soil moisture of the equal area cell, where
persistently frozen data , as determined by NNHIRS near air surface
temperature below 268K for the the day,is eliminated " ;
        vsm:references = "http://www.esa-soilmoisture-cci.org; Liu,
Y.Y., Dorigo, W.A., Parinussa, R.M., de Jeu, R.A.M. , Wagner, W., McCabe,
M.F., Evans, J.P., van Dijk, A.I.J.M. (2012). Trend-preserving blending of
passive and active microwave soil moisture retrievals, Remote Sensing of
Environment, 123, 280-297, doi: 10.1016/j.rse.2012.03.appendix014; Liu,
Y.Y., Parinussa, R.M., Dorigo, W.A., De Jeu, R.A.M., Wagner, W., van Dijk,
A.I.J.M., McCabe, M.F., & Evans, J.P. (2011): Developing an improved soil
moisture dataset by blending passive and active microwave satellite based
retrievals. Hydrology and Earth System Sciences, 15, 425-436; Wagner, W.,
W. Dorigo, R. de Jeu, D. Fernandez, J. Benveniste, E. Haas, M. Ertl
(2012): Fusion of active and passive microwave observations to create an
Essential Climate Variable data record on soil moisture. ISPRS Annals of
the Photogrammetry, Remote Sensing and Spatial Information Sciences,

```


Volume I-7, 2012. XXII ISPRS Congress, 25 August ,Äi 01 September 2012, Melbourne, Australia" ;

```

    ubyte vsmoflag(eqcell) ;
    vsmoflag:long_name = "Soil moisture origin flag" ;
    vsmoflag:flag_values = 0UB, 1UB, 2UB, 3UB, 4UB, 5UB, 6UB, 7UB,
255UB ;
    vsmoflag:flag_meaning = "original_data
snow_coverage_or_temperature_below_zero interpolated_data replicated_data
filled_with_maximum filled_with_climatology permanent_snow/glacier
undefined" ;
    short snowfrac(eqcell) ;
    snowfrac:long_name = "Fraction of equal-area grid covered with
snow" ;
    snowfrac:units = "1" ;
    snowfrac:scale_factor = 0.01f ;
    snowfrac:valid_min = 0 ;
    snowfrac:valid_max = 1 ;
    snowfrac:_FillValue = -9999s ;
    snowfrac:description = "Snow fraction determined from
microwave daily snow cover product (1998-2004) and the ISCCP daily snowice
product (2005 - 2007)" ;
    snowfrac:references =
"http://www.noacrest.org/LSH/snowcover.html;
http://www.noacrest.org/GGEWC/snowice.html" ;
    short FDtemps(times, eqcell) ;
    FDtemps:long_name = "Land surface skin temperature" ;
    FDtemps:units = "K" ;
    FDtemps:scale_factor = 0.1f ;
    FDtemps:valid_min = 165 ;
    FDtemps:valid_max = 355 ;
    FDtemps:_FillValue = -9999s ;
    FDtemps:description = " Surface skin temeprature is taken from
the ISCCP FD product" ;
    FDtemps:reference =
"http://www.ISCCP.giss.nasa.gov/projects/flux.html, Zhang, Y-C., W.B.
Rossow, A.A. Lacis, M.I. Mishchenko and V. Oinas,Calculation of radiative
fluxes from the surface to top-of-atmosphere\nbased on ISCCP and other
global datasets: Refinements of the radiative\ntransfer model and the
input data. J. Geophys. Res., 109, doi\n10.1029/2003JD004457 (1-27 + 1-
25), 2004." ;
    short presst(levels_t) ;
    presst:long_name = "Temperature pressure levels" ;
    presst:units = "hPa" ;
    presst:scale_factor = 0.1f ;
    presst:valid_min = 500. ;
    presst:valid_max = 1019 ;
    presst:description = "Pressure levels associated with
atmospheric temperature profile from the ISCCP NNHIRS product" ;
    presst:reference =
"http://www.noacrest.org/rscg/Products/GGEWC/NNHIRS.html" ;
    short pressrh(levels_t) ;
    pressrh:long_name = "Relative humidity pressure levels" ;

```

```

        pressrh:units = "hPa" ;
        pressrh:scale_factor = 0.1f ;
        pressrh:valid_min = 500. ;
        pressrh:valid_max = 1019 ;
        pressrh:description = "Pressure levels associated with
atmospheric relative humidity profile from the ISCCP NNHIRS product" ;
        pressrh:reference =
"http://www.noacrest.org/rscg/Products/GGEWC/NNHIRS.html" ;
        ubyte NNoflag(times, eqcell) ;
        NNoflag:long_name = "Origin code for NNHIRS" ;
        NNoflag:flag_values = 0UB, 1UB, 2UB, 3UB, 4UB, 5UB, 6UB, 7UB,
8UB, 255UB ;
        NNoflag:flag_meaning = "original daily-mean-pca 5d-daily-mean-
pca 30d-daily-mean-pca 8yr-daily-mean-pca daily-mean-nopca 5d-daily-mean-
nopca 30d-daily-mean-nopca 8yr-daily-mean-nopca no-data" ;
        NNoflag:reference =
"http://www.noacrest.org/rscg/Products/GGEWC/NNHIRS.html" ;
        short NNta(times, eqcell) ;
        NNta:long_name = "Near-surface air temperature (2 meters)" ;
        NNta:units = "Kelvin" ;
        NNta:scale_factor = 0.1f ;
        NNta:valid_min = 160 ;
        NNta:valid_max = 350 ;
        NNta:_FillValue = -9999s ;
        NNta:description = "Near surface air temperature from the
ISCCP NNHIRS product" ;
        NNta:reference =
"http://www.noacrest.org/rscg/Products/GGEWC/NNHIRS.html" ;
        short NNtprofile(times, eqcell, levels_t) ;
        NNtprofile:long_name = "Atmospheric temperature profile to 500
hPa" ;
        NNtprofile:units = "Kelvin" ;
        NNtprofile:scale_factor = 0.1f ;
        NNtprofile:valid_min = 160 ;
        NNtprofile:valid_max = 350 ;
        NNtprofile:_FillValue = -9999s ;
        NNtprofile:description = "Atmospheric temperature profile up
to 500hPa from the ISCCP NNHIRS product" ;
        NNtprofile:reference =
"http://www.noacrest.org/rscg/Products/GGEWC/NNHIRS.html" ;
        short tmax(times, eqcell) ;
        tmax:long_name = "Maximum temperature" ;
        tmax:units = "Kelvin" ;
        tmax:valid_min = 160 ;
        tmax:valid_max = 350 ;
        tmax:_FillValue = -9999s ;
        tmax:scale_factor = 0.1f ;
        tmax:descripton = "Maximum profile temperature from the ISCCP
NNHIRS product" ;
        tmax:reference =
"http://www.noacrest.org/rscg/Products/GGEWC/NNHIRS.html" ;
        short ttrop(times, eqcell) ;
        ttrop:long_name = "Tropopause temperature" ;
        ttrop:units = "Kelvin" ;

```

```

        ttrop:valid_min = 160 ;
        ttrop:valid_max = 350 ;
        ttrop:_FillValue = -9999s ;
        ttrop:scale_factor = 0.1f ;
        ttrop:descripton = "Tropopause temperature from the ISCCP
NNHIRS product" ;
        ttrop:reference =
"http://www.noacrest.org/rscg/Products/GGEWC/NNHIRS.html" ;
        short psurf(times, eqcell) ;
        psurf:long_name = "Surface pressure" ;
        psurf:units = "hPa" ;
        psurf:valid_min = 10 ;
        psurf:valid_max = 1019 ;
        psurf:_FillValue = -9999s ;
        psurf:scale_factor = 0.1f ;
        psurf:descripton = "Surface pressure from the ISCCP NNHIRS
product" ;
        psurf:reference =
"http://www.noacrest.org/rscg/Products/GGEWC/NNHIRS.html" ;
        short pmxt(times, eqcell) ;
        pmxt:long_name = "Pressure at max temperature" ;
        pmxt:units = "percent" ;
        pmxt:valid_min = 10 ;
        pmxt:valid_max = 1019 ;
        pmxt:_FillValue = -9999s ;
        pmxt:scale_factor = 0.1f ;
        pmxt:descripton = "Pressure at maximum profile temperature
from the ISCCP NNHIRS product" ;
        pmxt:reference =
"http://www.noacrest.org/rscg/Products/GGEWC/NNHIRS.html" ;
        short ptrop(times, eqcell) ;
        ptrop:long_name = "Pressure at tropopause" ;
        ptrop:units = "percent" ;
        ptrop:valid_min = 10 ;
        ptrop:valid_max = 1019 ;
        ptrop:_FillValue = -9999s ;
        ptrop:scale_factor = 0.1f ;
        ptrop:descripton = "Pressure at tropopause from the ISCCP
NNHIRS product" ;
        ptrop:reference =
"http://www.noacrest.org/rscg/Products/GGEWC/NNHIRS.html" ;
        short NNrha(times, eqcell) ;
        NNrha:long_name = "Near-surface relative humidity" ;
        NNrha:units = "percent" ;
        NNrha:valid_min = 0.5 ;
        NNrha:valid_max = 150. ;
        NNrha:_FillValue = -9999s ;
        NNrha:scale_factor = 0.01f ;
        NNrha:descripton = "Near-surface relative humidity from the
ISCCP NNHIRS product" ;
        NNrha:reference =
"http://www.noacrest.org/rscg/Products/GGEWC/NNHIRS.html" ;

```

```

    short NNrhprof(times, eqcell, levels_t) ;
        NNrhprof:long_name = "Relative humidity profile up to 500 hPa"
;
        NNrhprof:units = "percent" ;
        NNrhprof:valid_min = 0.5 ;
        NNrhprof:valid_max = 150. ;
        NNrhprof:_FillValue = -9999s ;
        NNrhprof:scale_factor = 0.01f ;
        NNrhprof:description = " Relative humidity profile up to 500
hPa from the ISCCP NNHIRS product" ;
        NNrhprof:reference =
"http://www.noacrest.org/rscg/Products/GGEWC/NNHIRS.html" ;
    short NNrhmaxt(times, eqcell) ;
        NNrhmaxt:long_name = "Relative humidity at max temperature" ;
        NNrhmaxt:units = "percent" ;
        NNrhmaxt:valid_min = 0.5 ;
        NNrhmaxt:valid_max = 150. ;
        NNrhmaxt:_FillValue = -9999s ;
        NNrhmaxt:scale_factor = 0.01f ;
        NNrhmaxt:description = "Relative humidity at max temperature
from the ISCCP NNHIRS product" ;
        NNrhmaxt:reference =
"http://www.noacrest.org/rscg/Products/GGEWC/NNHIRS.html" ;
    short NNrhtrop(times, eqcell) ;
        NNrhtrop:long_name = "Relative humidity at tropopause" ;
        NNrhtrop:units = "percent" ;
        NNrhtrop:valid_min = 0.5 ;
        NNrhtrop:valid_max = 150. ;
        NNrhtrop:_FillValue = -9999s ;
        NNrhtrop:scale_factor = 0.01f ;
        NNrhtrop:description = "Relative humidity at tropopause from
the ISCCP NNHIRS product" ;
        NNrhtrop:reference =
"http://www.noacrest.org/rscg/Products/GGEWC/NNHIRS.html" ;
    short ISDwspeed(times, eqcell) ;
        ISDwspeed:long_name = "Station wind speed" ;
        ISDwspeed:units = "m s-1" ;
        ISDwspeed:_FillValue = -9999s ;
        ISDwspeed:scale_factor = 0.1f ;
        ISDwspeed:description = "Surface wind speed retrieved from the
Integrated Surface Database" ;
        ISDwspeed:reference = "https://www.ncdc.noaa.gov/isd,
Smith,A., N. Lott and R.Vose, 2011: The Integrated Surface Database:
Recent developments and partnerships. Bull. Amer. Meteor. Soc., 92, 704-
708, doi:10.1175/2011BAMS3015.1." ;
    ubyte ISDwflag(times, eqcell) ;
        ISDwflag:long_name = "Station wind origin code" ;
        ISDwflag:flag_values = 1UB, 2UB, 3UB, 4UB, 5UB, 6UB, 255UB ;
        ISDwflag:flag_meaning = "original_value interpolated_value
replicated_value filled_with_2.5_degree filled_with_5.0_degree undefined
undefined" ;
    short ISDwcount(times, eqcell) ;
        ISDwcount:long_name = "Number of stations used to calculate
the wind speed" ;

```

```

        ISDwcount:units = "1" ;
        ISDwcount:_FillValue = -9999s ;
        ISDwcount:description = "Number of stations used to calculate
the wind speed average for each equal-area grid cell" ;
        short ISDta(times, eqcell) ;
        ISDta:long_name = "Near-surface air temperature from the ISD
collection" ;
        ISDta:units = "Kelvin" ;
        ISDta:scale_factor = 0.1f ;
        ISDta:valid_min = 160 ;
        ISDta:valid_max = 350 ;
        ISDta:_FillValue = -9999s ;
        ISDta:description = "Near-surface air temperature retrieved
from the Integrated Surface Database" ;
        ISDta:reference = "https://www.ncdc.noaa.gov/isd,Smith,A., N.
Lott and R.Vose, 2011: The Integrated Surface Database: Recent
developments and partnerships. Bull. Amer. Meteor. Soc., 92, 704-708,
doi:10.1175/2011BAMS3015.1. " ;
        ubyte ISDtaflag(times, eqcell) ;
        ISDtaflag:long_name = "Near-surface air temperature origin
code" ;
        ISDtaflag:flag_values = 0UB, 1UB, 2UB, 3UB, 4UB, 5UB, 255UB ;
        ISDtaflag:flag_meaning = "original_value interpolated_value
replicated_value filled_with_2.5_degree filled_with_5.0_degree undefined "
;
        short ISDtacount(times, eqcell) ;
        ISDtacount:long_name = "Number of stations used to calculate
the air temperature average" ;
        ISDtacount:units = "1" ;
        ISDtacount:_FillValue = -9999s ;
        ISDtacount:description = "Number of stations used to calculate
the air temperature average for each equal-area grid cell" ;
        short ISDrha(times, eqcell) ;
        ISDrha:long_name = "Near-surface air relative_humidity from
the ISD collection" ;
        ISDrha:units = "percent" ;
        ISDrha:scale_factor = 0.1f ;
        ISDrha:valid_min = 0.5 ;
        ISDrha:valid_max = 110. ;
        ISDrha:_FillValue = -9999s ;
        ISDrha:description = "Near-surface air relative humidity from
the Integrated Surface Database" ;
        ISDrha:reference = "https://www.ncdc.noaa.gov/isdm, Smith,A.,
N. Lott and R.Vose, 2011: The Integrated Surface Database: Recent
developments and partnerships. Bull. Amer. Meteor. Soc., 92, 704-708,
doi:10.1175/2011BAMS3015.1." ;
        ubyte ISDrhflag(times, eqcell) ;
        ISDrhflag:long_name = "Near-surface air relative humidity
origin code" ;
        ISDrhflag:flag_values = 1UB, 2UB, 3UB, 4UB, 5UB, 255UB ;

```

```

        ISDrhflag:flag_meaning = "original_value interpolated_value
replicated_value filled_with_2.5_degree filled_with_5.0_degree undefined "
;
        short ISDrhcount(times, eqcell) ;
        ISDrhcount:long_name = "Number of stations used to calculate
the relative humidity average" ;
        ISDrhcount:_FillValue = -9999s ;
        ISDrhcount:units = "1" ;
        ISDrhcount:description = "Number of stations used to calculate
the near surface air relative humidity average for each equal-area grid
cell" ;
        short preciprate(times, eqcell) ;
        preciprate:long_name = "Precipitation rate" ;
        preciprate:units = "mm/hour" ;
        preciprate:_FillValue = -9999s ;
        preciprate:scale_factor = 0.01f ;
        preciprate:_description = "Hourly precipitation rate
from merged GPCP and TMPA data" ;
        preciprate:references = "Huffman, G.J., R.F. Adler, M.M.
Morrissey, S. Curtis \nR. Joyce, B. McGavock, and J. Susskind, 2001:
\n ftp://meso.gfsc.nasa.gov/pub/1dd-v1.\n Global precipitation at one-
degree daily resolution from multi-satellite observations\n
http://pmm.nasa.gov/data-access/downloads/trmm/\n" ;
        short precipratio(times, eqcell) ;
        precipratio:long_name = "Precipitation ratio" ;
        precipratio:units = "1" ;
        precipratio:_FillValue = -9999s ;
        precipratio:valid_max = 1. ;
        precipratio:scale_factor = 0.01f ;
        precipratio:valid_min = 0 ;
        precipratio:description = "Ratio of the precipitation rate
including 0 to the precipitation rate without 0" ;
        ubyte precipoflag(times, eqcell) ;
        precipoflag:long_name = " Precipitation origin flag " ;
        precipoflag:units = "1" ;
        precipoflag:flag_meaning = "TMPA GPCP undefined" ;
        precipoflag:flag_values = 0UB, 1UB, 255UB ;
        precipoflag:description = "Origin flag of the precipitation
data" ;
        ubyte preciptflag(times, eqcell) ;
        preciptflag:long_name = "Precipitation type flag" ;
        preciptflag:units = "1" ;
        preciptflag:_FillValue = 255UB ;
        preciptflag:flag_meaning = "liquid frozen undefined" ;
        preciptflag:flag_values = 0UB, 1UB, 255UB ;
        preciptflag:_description = "Flag indicates whether precipitation
for a given cell is liquid or frozen which is determined by air surface
temperature of less than 268 K found in the NNHIRS retrieval" ;
        char lctlable(low_cloud_type, label_len) ;
        lctlable:long_name = "Low cloud type labels" ;
        lctlable:units = "1" ;
        lctlable:description = "Low cloud type label as determined
where uppermost cloud top pressure is greater than 500 hPa" ;
        short lcfrac(times, eqcell, low_cloud_type) ;

```

```

        lcfrac:long_name = "Low cloud fraction" ;
        lcfrac:units = "1" ;
        lcfrac:valid_min = 0 ;
        lcfrac:valid_max = 1 ;
        lcfrac:_FillValue = -9999s ;
        lcfrac:scale = 0.01 ;
        lcfrac:description = "Low cloud fraction from the ISCCP FD
dataset where cloud top is less than 500 hPa" ;
        lcfrac:reference =
"http://www.ISCCP.giss.nasa.gov/projects/flux.html, , Zhang, Y-C., W.B.
Rossow, A.A. Lacis, M.I. Mishchenko and V. Oinas,\nCalculation of
radiative fluxes from the surface to top-of-atmosphere\nbased on ISCCP and
other global datasets: Refinements of the radiative\ntransfer model and
the input data. J. Geophys. Res., 109, doi\n10.1029/2003JD004457 (1-27 +
1-25), 2004." ;
        short dccfrac(times, eqcell) ;
        dccfrac:long_name = "Deep convective cloud fraction" ;
        dccfrac:units = "1" ;
        dccfrac:valid_min = 0 ;
        dccfrac:valid_max = 1 ;
        dccfrac:_FillValue = -9999s ;
        dccfrac:scale = 0.01 ;
        dccfrac:description = "Cloud fraction from theISCCP FD dataset
where base pressure is less than 440 hPa and cloud opticalthickness is
greater than 23" ;
        dccfrac:reference =
"http://www.ISCCP.giss.nasa.gov/projects/flux.html, , Zhang, Y-C., W.B.
Rossow, A.A. Lacis, M.I. Mishchenko and V. Oinas,\nCalculation of
radiative fluxes from the surface to top-of-atmosphere\nbased on ISCCP and
other global datasets: Refinements of the radiative\ntransfer model and
the input data. J. Geophys. Res., 109, doi\n10.1029/2003JD004457 (1-27 +
1-25), 2004." ;
        short clbasep(times, eqcell) ;
        clbasep:long_name = "Lowermost cloud base pressure" ;
        clbasep:units = "hPa" ;
        clbasep:scale_factor = 0.01f ;
        clbasep:_FillValue = -9999s ;
        clbasep:valid_min = 10. ;
        clbasep:valid_max = 1019. ;
        clbasep:description = "Lower most cloud base pressure where
cloud top is less than 500 hPa" ;
        clbasep:reference =
"http://www.ISCCP.giss.nasa.gov/projects/flux.html" ;
        short cltopp(times, eqcell) ;
        cltopp:long_name = "Uppermost cloud top pressure" ;
        cltopp:units = "hPa" ;
        cltopp:scale_factor = 0.01f ;
        cltopp:_FillValue = -9999s ;
        cltopp:valid_min = 10. ;
        cltopp:valid_max = 1019. ;
        cltopp:description = "Upper most cloud top pressure where
cloud top is less than 500 hPa" ;

```

```

        cltopp:reference =
"http://www.ISCCP.giss.nasa.gov/projects/flux.html,, Zhang, Y-C., W.B.
Rossow, A.A. Lacis, M.I. Mishchenko and V. Oinas,\nCalculation of
radiative fluxes from the surface to top-of-atmosphere\nbased on ISCCP and
other global datasets: Refinements of the radiative\ntransfer model and
the input data. J. Geophys. Res., 109, doi\n10.1029/2003JD004457 (1-27 +
1-25), 2004. " ;
        short totclfrac(times, eqcell) ;
        totclfrac:long_name = "Total cloud fraction" ;
        totclfrac:units = "1" ;
        totclfrac:scale_factor = 0.01f ;
        totclfrac:_FillValue = -9999s ;
        totclfrac:valid_min = 0 ;
        totclfrac:valid_max = 1. ;
        totclfrac:description = "Total Cloud Fraction form the ISCCP
FD dataset" ;
        totclfrac:reference =
"http://www.ISCCP.giss.nasa.gov/projects/flux.html,, Zhang, Y-C., W.B.
Rossow, A.A. Lacis, M.I. Mishchenko and V. Oinas,\nCalculation of
radiative fluxes from the surface to top-of-atmosphere\nbased on ISCCP and
other global datasets: Refinements of the radiative\ntransfer model and
the input data. J. Geophys. Res., 109, doi\n10.1029/2003JD004457 (1-27 +
1-25), 2004. " ;
        float swsurfflux(times, eqcell) ;
        swsurfflux:long_name = "Net short wave surface flux" ;
        swsurfflux:units = "W/ m^2" ;
        swsurfflux:_FillValue = -9999.f ;
        swsurfflux:Description = "Full sky surface short wave flux up
- full sky surface short wave flux down" ;
        swsurfflux:reference =
"http://www.ISCCP.giss.nasa.gov/projects/flux.html, , Zhang, Y-C., W.B.
Rossow, A.A. Lacis, M.I. Mishchenko and V. Oinas,\nCalculation of
radiative fluxes from the surface to top-of-atmosphere\nbased on ISCCP and
other global datasets: Refinements of the radiative\ntransfer model and
the input data. J. Geophys. Res., 109, doi\n10.1029/2003JD004457 (1-27 +
1-25), 2004." ;
        float lwsurfflux(times, eqcell) ;
        lwsurfflux:long_name = "Net long wave surface flux" ;
        lwsurfflux:units = "W/ m^2" ;
        lwsurfflux:_FillValue = -9999.f ;
        lwsurfflux:Description = "Full sky surface Long wave flux up -
full sky surface Long wave flux down" ;
        lwsurfflux:reference =
"http://www.ISCCP.giss.nasa.gov/projects/flux.html, , Zhang, Y-C., W.B.
Rossow, A.A. Lacis, M.I. Mishchenko and V. Oinas,\nCalculation of
radiative fluxes from the surface to top-of-atmosphere\nbased on ISCCP and
other global datasets: Refinements of the radiative\ntransfer model and
the input data. J. Geophys. Res., 109, doi\n10.1029/2003JD004457 (1-27 +
1-25), 2004." ;
        float sw680flux(times, eqcell) ;
        sw680flux:long_name = "Net short Wwave flux at 680 hPa" ;
        sw680flux:units = "W/ m^2" ;
        sw680flux:_FillValue = -9999.f ;

```



```

        sw680flux:Description = "Full sky short wave flux down - full
short wave flux up at 680 hPa" ;
        sw680flux:reference =
"http://www.ISCCP.giss.nasa.gov/projects/flux.html,, Zhang, Y-C., W.B.
Rossow, A.A. Lacis, M.I. Mishchenko and V. Oinas,\nCalculation of
radiative fluxes from the surface to top-of-atmosphere\nbased on ISCCP and
other global datasets: Refinements of the radiative\ntransfer model and
the input data. J. Geophys. Res., 109, doi\n10.1029/2003JD004457 (1-27 +
1-25), 2004. " ;
        float lw680flux(times, eqcell) ;
        lw680flux:long_name = "Net long wave flux at 680 hPa" ;
        lw680flux:units = "W/ m^2" ;
        lw680flux:_FillValue = -9999.f ;
        lw680flux:Description = "Full sky Long wave flux down - full
sky Long wave flux up at 680 hPa" ;
        lw680flux:reference =
"http://www.ISCCP.giss.nasa.gov/projects/flux.html, , Zhang, Y-C., W.B.
Rossow, A.A. Lacis, M.I. Mishchenko and V. Oinas,\nCalculation of
radiative fluxes from the surface to top-of-atmosphere\nbased on ISCCP and
other global datasets: Refinements of the radiative\ntransfer model and
the input data. J. Geophys. Res., 109, doi\n10.1029/2003JD004457 (1-27 +
1-25), 2004." ;
        short FDta(times, eqcell) ;
        FDta:long_name = "Near-surface air temperature from the FD
dataset" ;
        FDta:units = "Kelvin" ;
        FDta:scale_factor = 0.1 ;
        FDta:valid_min = 160 ;
        FDta:valid_max = 350 ;
        FDta:_FillValue = -9999s ;
        FDta:Description = "Near-surface air temperature from the FD
dataset" ;
        FDta:reference =
"http://www.ISCCP.giss.nasa.gov/projects/flux.html, , Zhang, Y-C., W.B.
Rossow, A.A. Lacis, M.I. Mishchenko and V. Oinas,\nCalculation of
radiative fluxes from the surface to top-of-atmosphere\nbased on ISCCP and
other global datasets: Refinements of the radiative\ntransfer model and
the input data. J. Geophys. Res., 109, doi\n10.1029/2003JD004457 (1-27 +
1-25), 2004." ;
        float ET_tran_liquid(eqcell) ;
        ET_tran_liquid:long_name = "Contribution to ET from
transpiration" ;
        ET_tran_liquid:units = "W/m2" ;
        ET_tran_liquid:_FillValue = -9999.f ;
        ET_tran_liquid:reference =
"http://hydrology.priceton.edu/data/landflux/et_prod" ;
        float ET_soil_liquid(eqcell) ;
        ET_soil_liquid:long_name = "Contribution to ET from soil
evaporation" ;
        ET_soil_liquid:units = "W/m2" ;
        ET_soil_liquid:_FillValue = -9999.f ;

```

```

        ET_soil_liquid:reference =
"http://hydrology.priceton.edu/data/landflux/et_prod" ;
        float ET_water_liquid(eqcell) ;
        ET_water_liquid:long_name = "Contribution to ET from open
water" ;
        ET_water_liquid:units = "W/m2" ;
        ET_water_liquid:_FillValue = -9999.f ;
        ET_water_liquid:reference =
"http://hydrology.priceton.edu/data/landflux/et_prod" ;
        float can_evap_liquid(eqcell) ;
        can_evap_liquid:long_name = "Evaporation from wet canopy" ;
        can_evap_liquid:units = "W/m2" ;
        can_evap_liquid:_FillValue = -9999.f ;
        can_evap_liquid:reference =
"http://hydrology.priceton.edu/data/landflux/et_prod" ;
        float ET_snow_liquid(eqcell) ;
        ET_snow_liquid:long_name = "Evaporation from snow" ;
        ET_snow_liquid:units = "W/m2" ;
        ET_snow_liquid:_FillValue = -9999.f ;
        ET_snow_liquid:reference =
"http://hydrology.priceton.edu/data/landflux/et_prod" ;
        ubyte ET_type_flag(eqcell) ;
        ET_type_flag:long_name = "ET type flag" ;
        ET_type_flag:units = "1" ;
        ET_type_flag:flag_meaning = "liquid frozen undefined" ;
        ET_type_flag:flag_values = 0UB, 1UB, 255UB ;
        ET_type_flag:_description = "Flag indicates whether ET for a
given cell is liquid or frozen which is determined by a daily air surface
temperature of less then 268 K found in the NNHIRS retrieval" ;

// global attributes:
        :Conventions = "CF-1.4" ;
        :title = "Land Surface Meteorology data" ;
        :author = "William B. Rossow" ;
        :producer = "William B. Rossow" ;
        :institution = "The City College of New York NOAA/CREST" ;
        :first_release_date = "November 2016" ;
        :source = "Multiple Observational Sources" ;
        :citation = "TBD" ;
        :references = "TBD" ;
        :identifier_product_DOI = "10.5067/MEASURES/LANDMET/DATA001" ;
        :identifier_product_DOI_authority = "http://dx.doi.org/" ;
        :comment = "Version one produced at CCNY" ;
        :processing_level = "3" ;
        :range_beginning_time = "00:00:00" ;
        :range_ending_time = "23:59:59" ;
        :short_name = "LANDMET" ;
        :long_name = "Land Surface Atmospheric Boundary Interaction
Product L3" ;
        :format = "netCDF-4 classic" ;
        :version_id = "1" ;
        :year = 2003 ;
        :month = 1 ;
        :day = 1 ;

```

```
    :production_run_date = "2016-11-16" ;  
    :production_run_time = "08:29:31" ;  
    :range_beginning_date = "2003-01-01" ;  
    :range_ending_date = "2003-01-01" ;  
    :granule_id = "landmet_L3_20030101_v1.nc" ;  
}
```

8. Appendix – Sample Images for Each Variable from 2003 01 01

By applying the following pseudo code an equal-area grid image can be represented as an equal-angle grid.

Retrieve variables from the netcdf file (In this example the physical variable is ttrop):

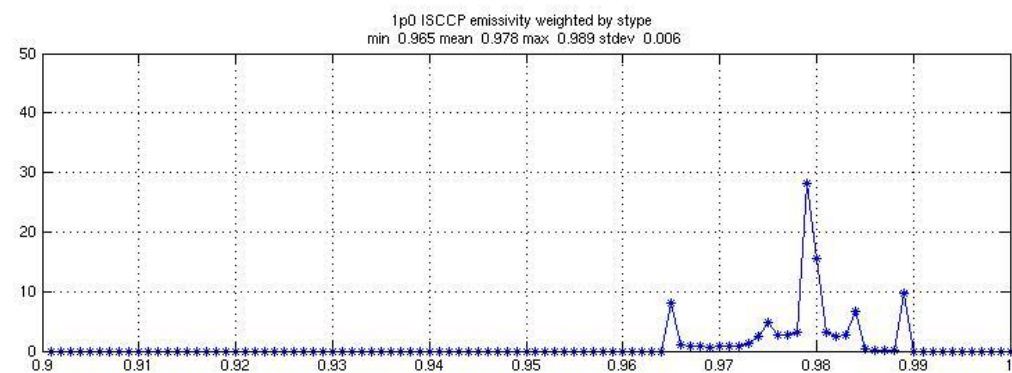
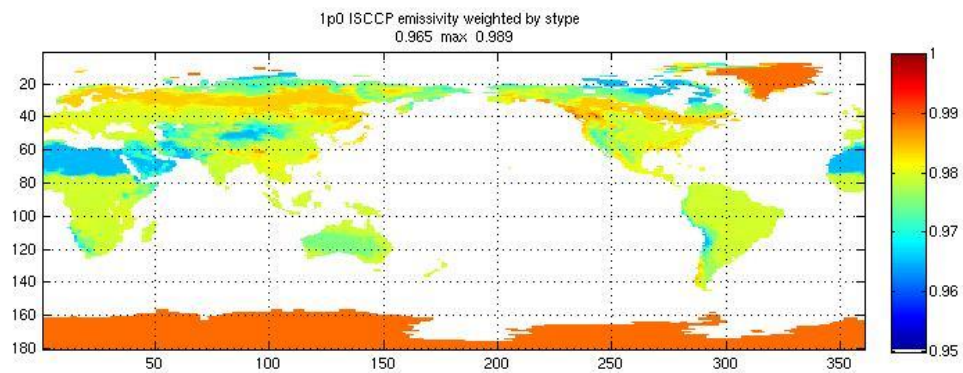
```
sqlon_beg,  
sqlon_end,  
eqlat_index  
eqcell  
ttrop  
  
do icell=1,eqcell  
  ilon1 = sqlon_beg(icell)  
  ilon2 = sqlon_end(icell)  
  ilat = eqlat_index(icell)  
  do i=ilon1,ilon2  
    sqmap(i,ilat) = ttrop(icell)  
  enddo  
enddo
```

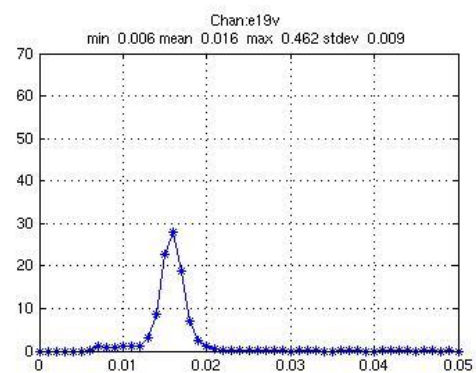
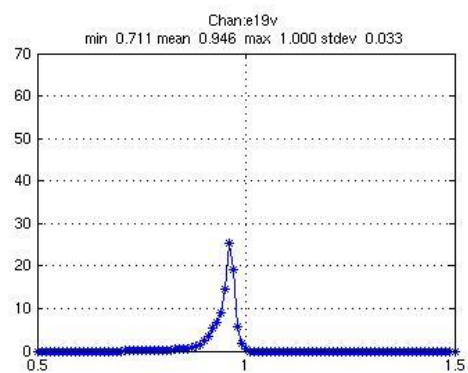
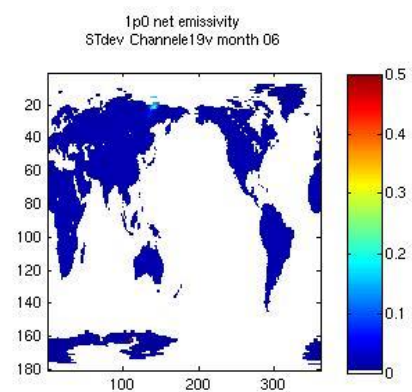
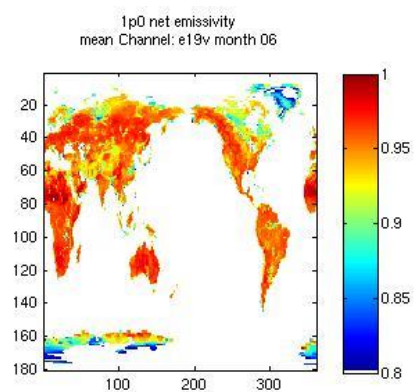
The variable *sqmap(360,180)* can now be displayed in equal angle format.

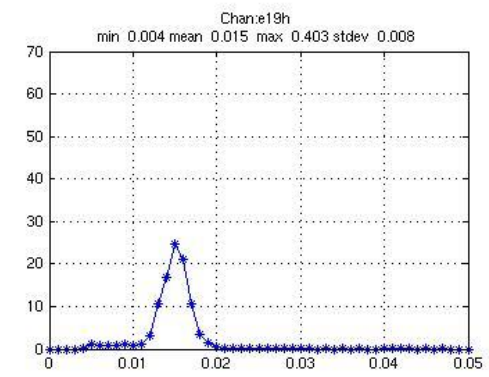
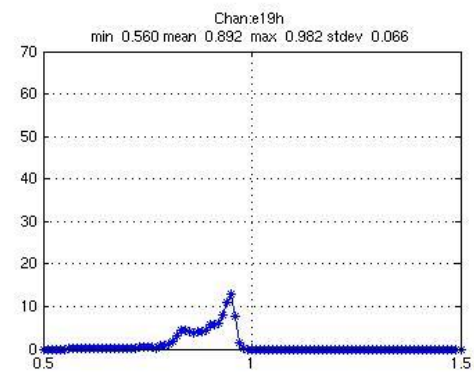
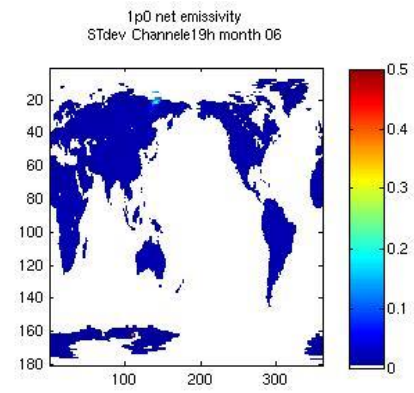
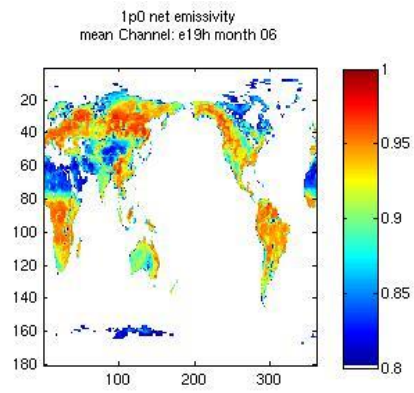
The following figures show 1 equal angle map and one histogram for each equal area grid variable found in the 20030101 LandMet netcdf file and the ancillary files.

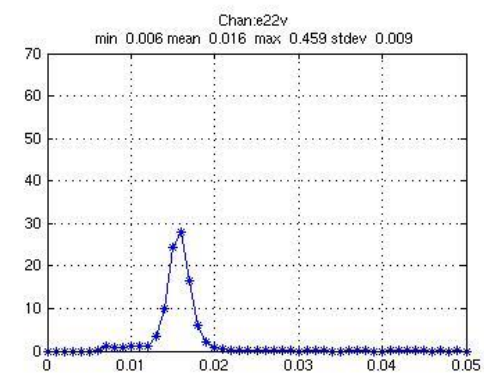
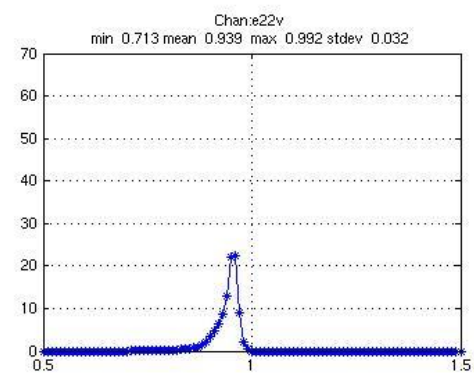
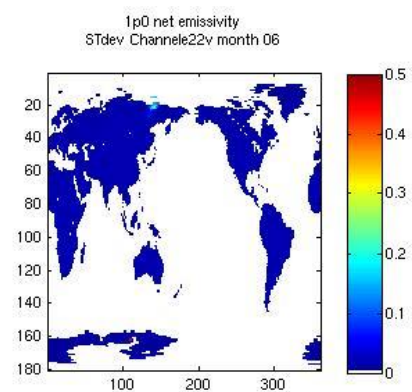
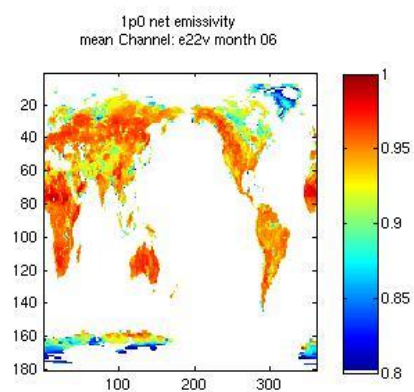
ALL Figures are for 20030101

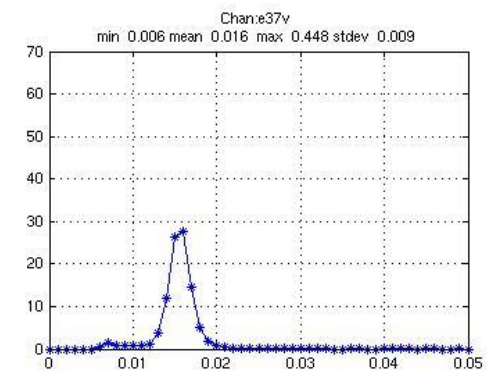
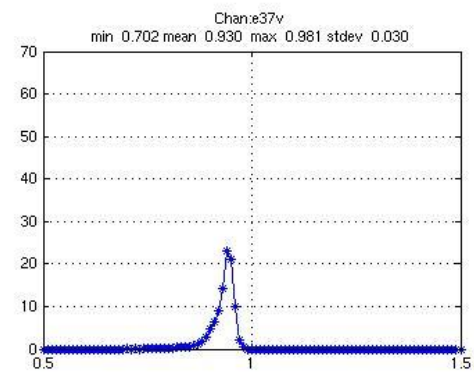
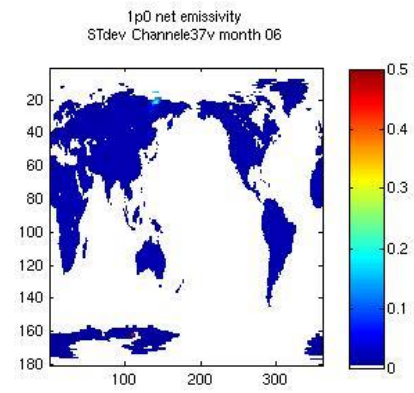
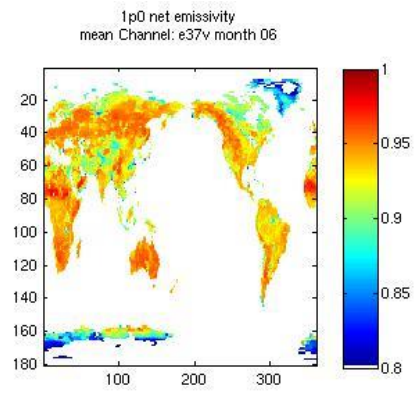
Emissivity ancillary file:

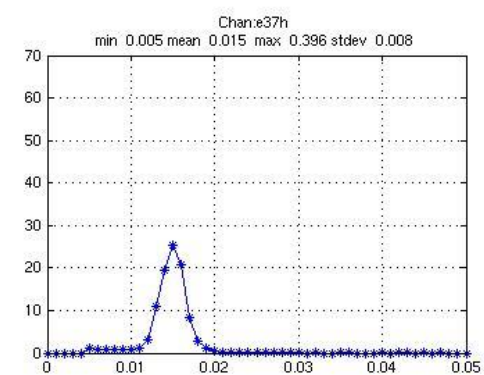
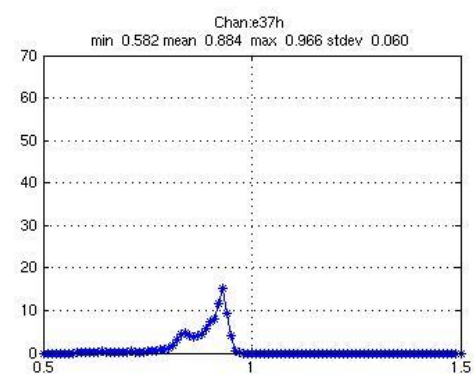
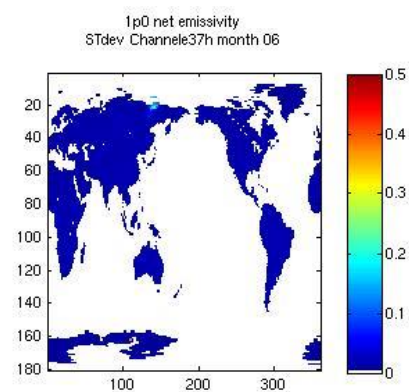
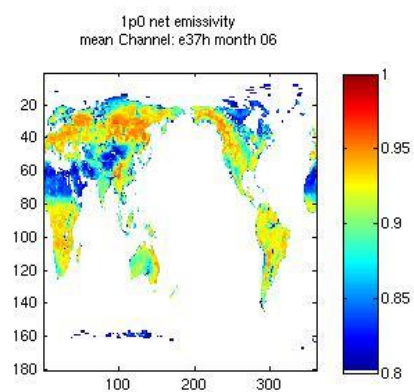


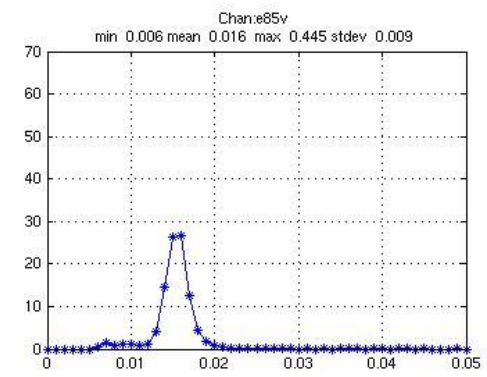
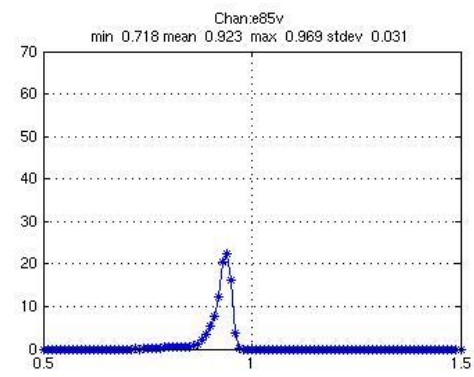
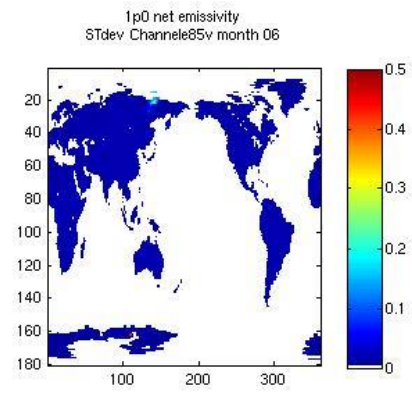
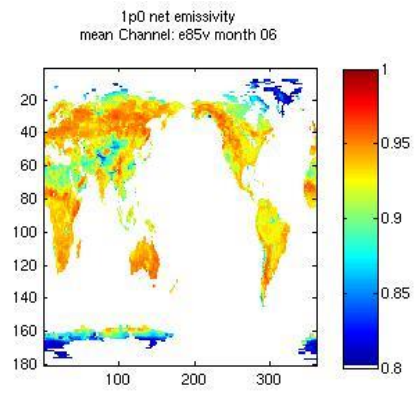


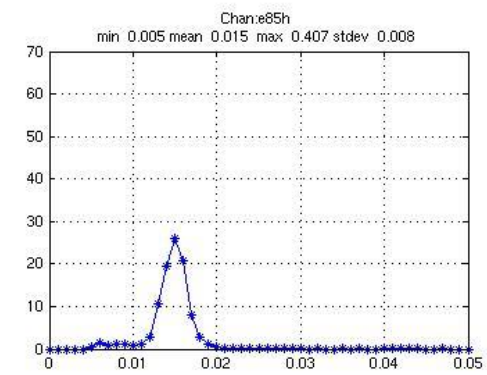
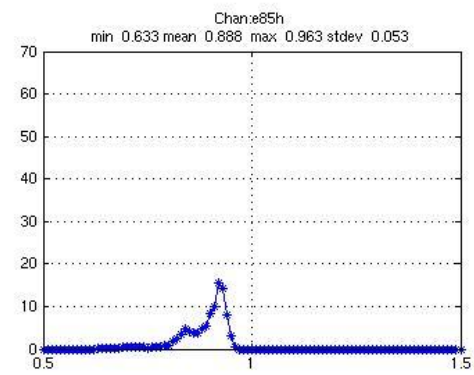
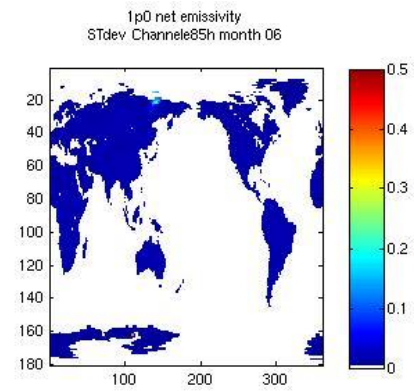
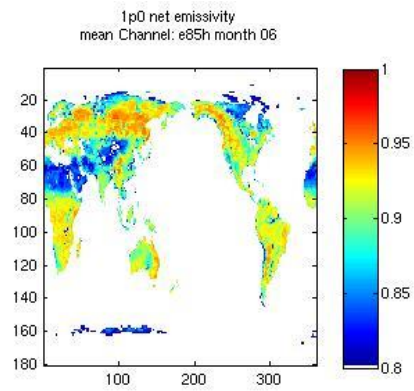


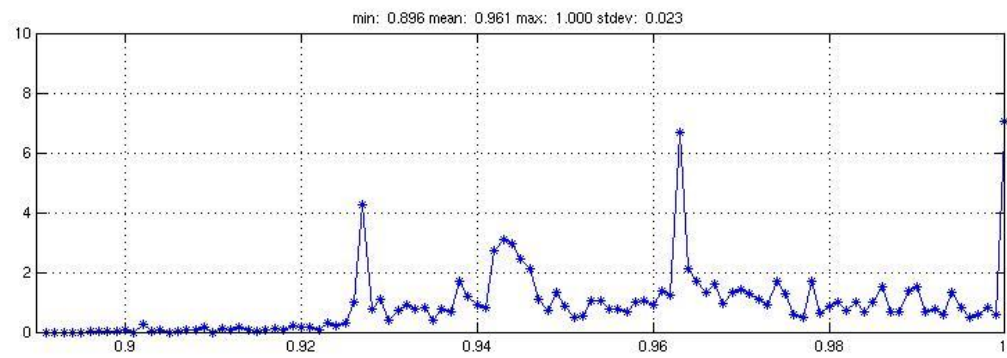
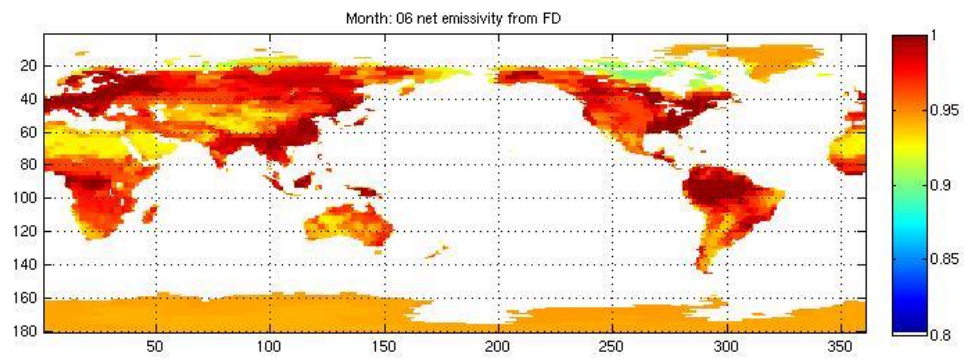






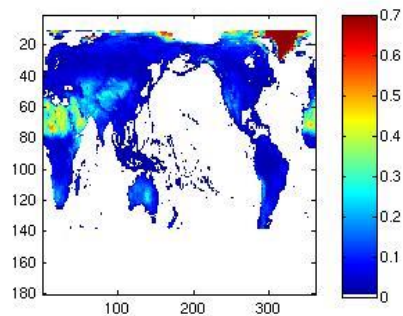




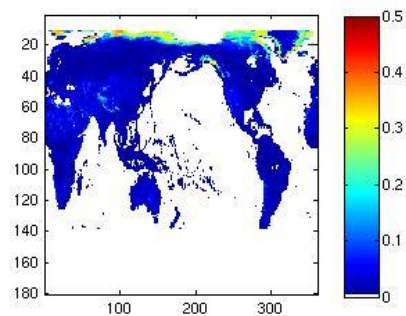


Ancillary Albedo

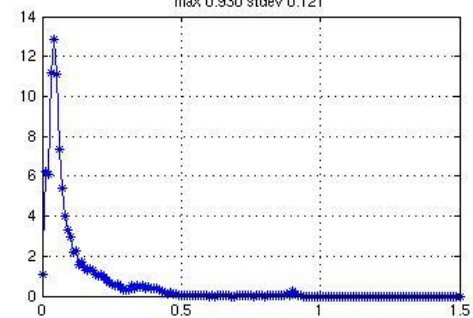
mean
MODIS bsa Albedo Map 0.659 month 06



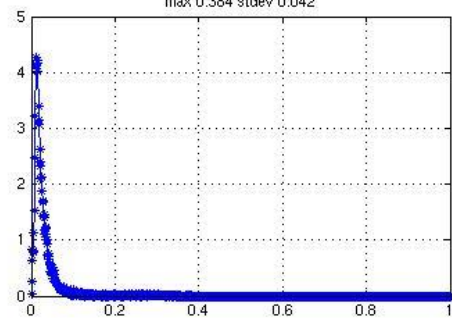
STDEV
MODIS bsa Albedo Map 0.659 month 06



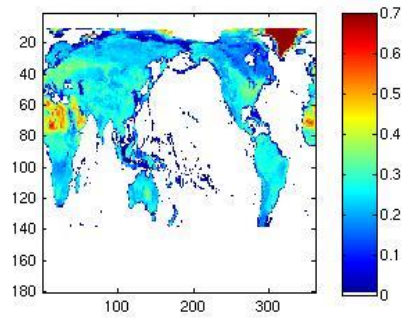
mean
min 0.001 mean 0.102
max 0.930 stdev 0.121



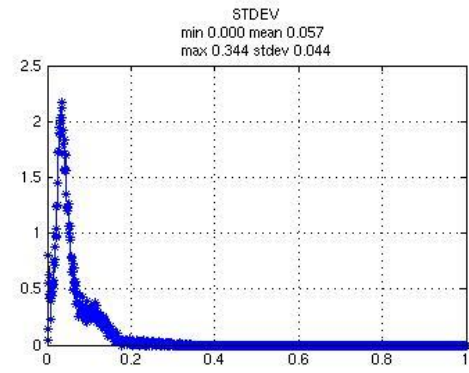
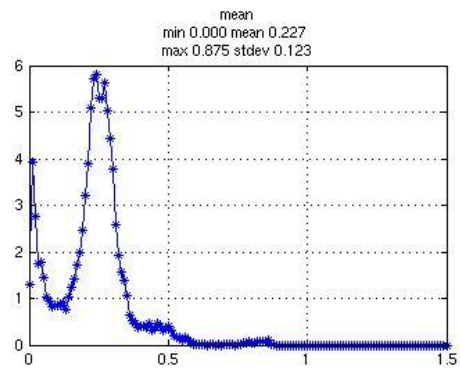
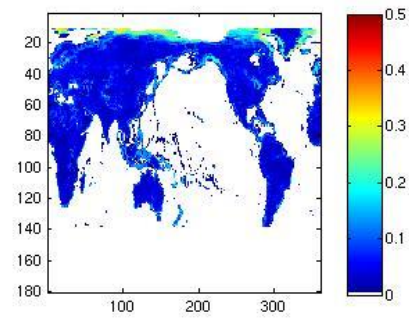
STDEV
min 0.000 mean 0.031
max 0.384 stdev 0.042



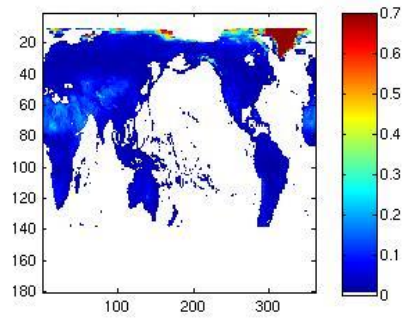
mean
MODIS bsa Albedo Map 0.858 month 06



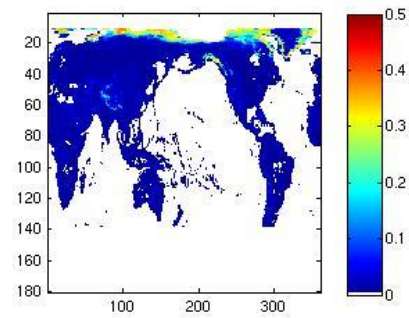
STDEV
MODIS bsa Albedo Map 0.858 month 06



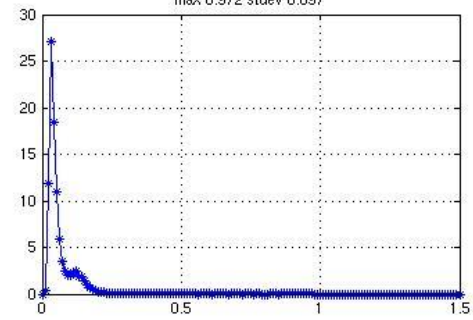
mean
MODIS bsa Albedo Map 0.47 month 06



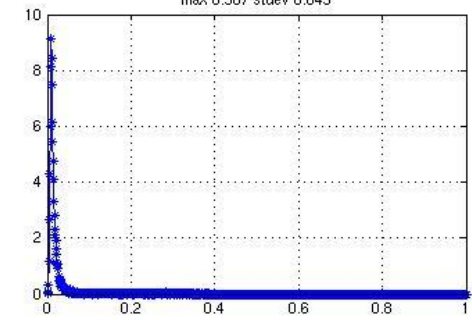
STDEV
MODIS bsa Albedo Map 0.47 month 06

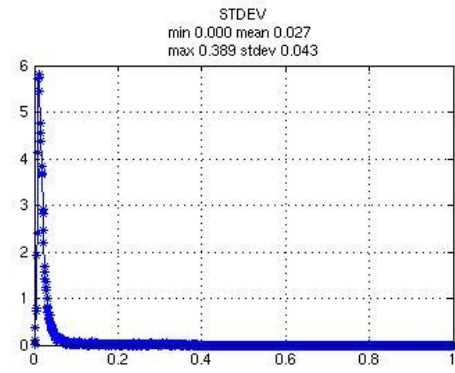
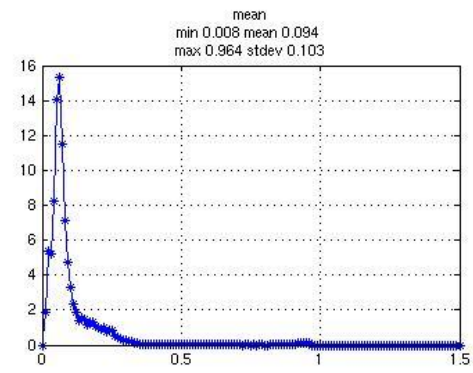
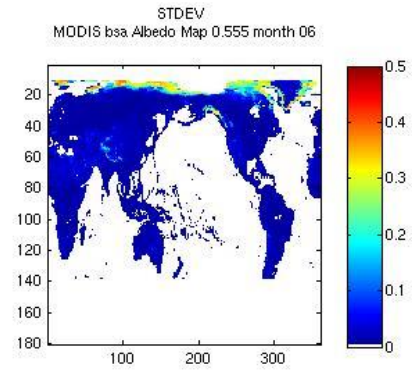
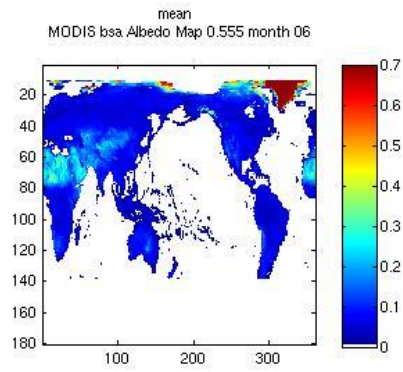


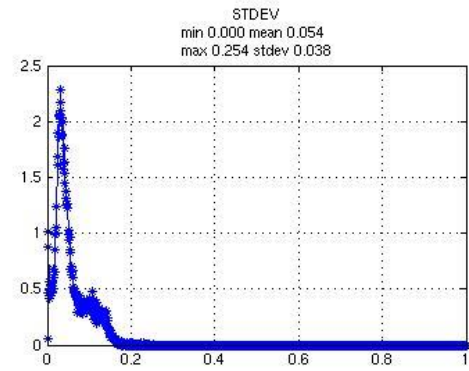
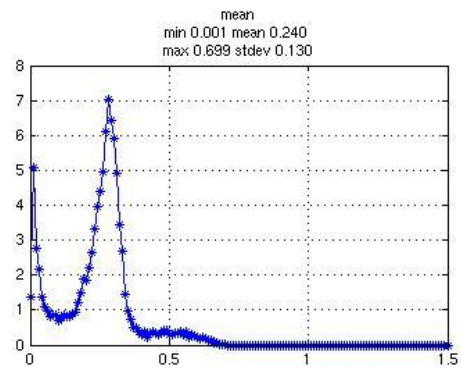
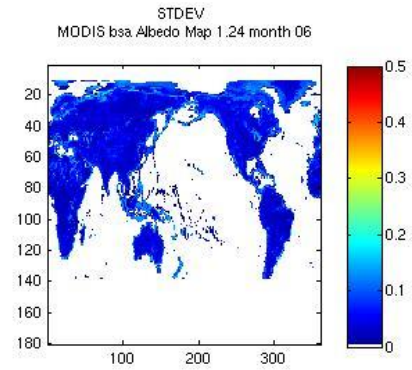
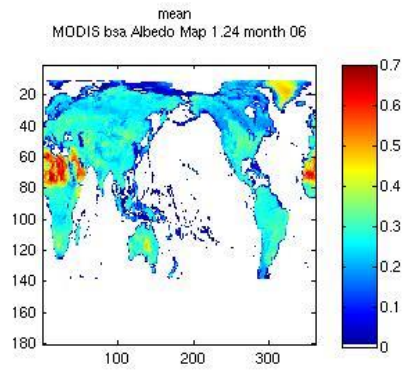
mean
min 0.010 mean 0.066
max 0.972 stdev 0.097



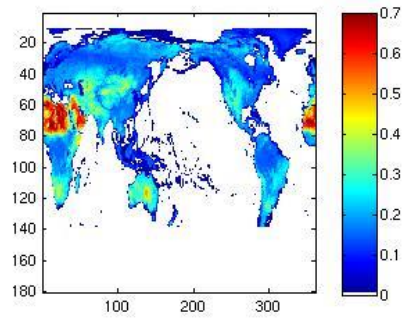
STDEV
min 0.000 mean 0.022
max 0.387 stdev 0.043



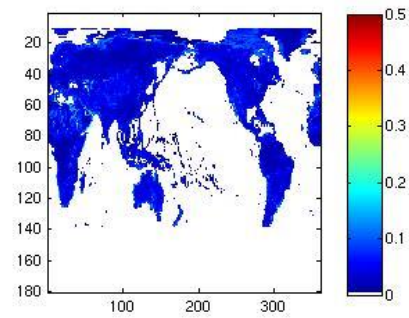




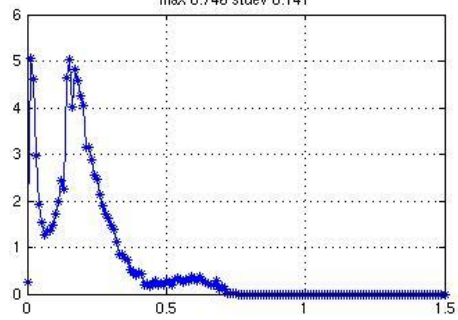
mean
MODIS bsa Albedo Map 1.64 month 06



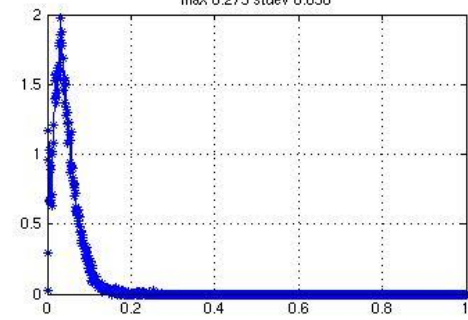
STDEV
MODIS bsa Albedo Map 1.64 month 06



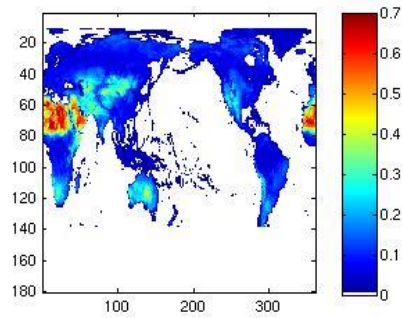
mean
min 0.003 mean 0.197
max 0.746 stdev 0.141



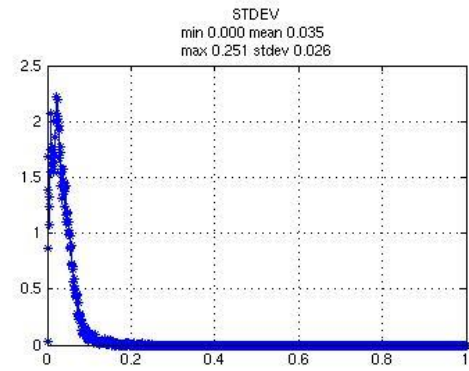
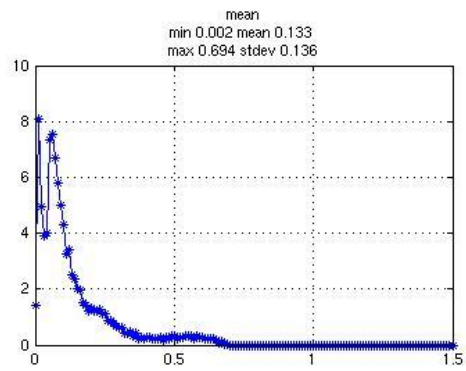
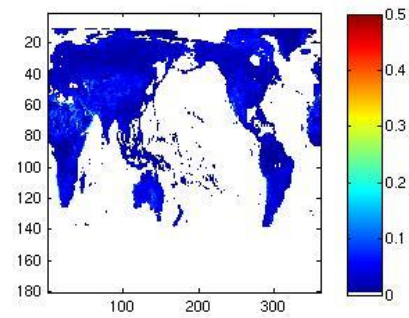
STDEV
min 0.000 mean 0.044
max 0.273 stdev 0.030

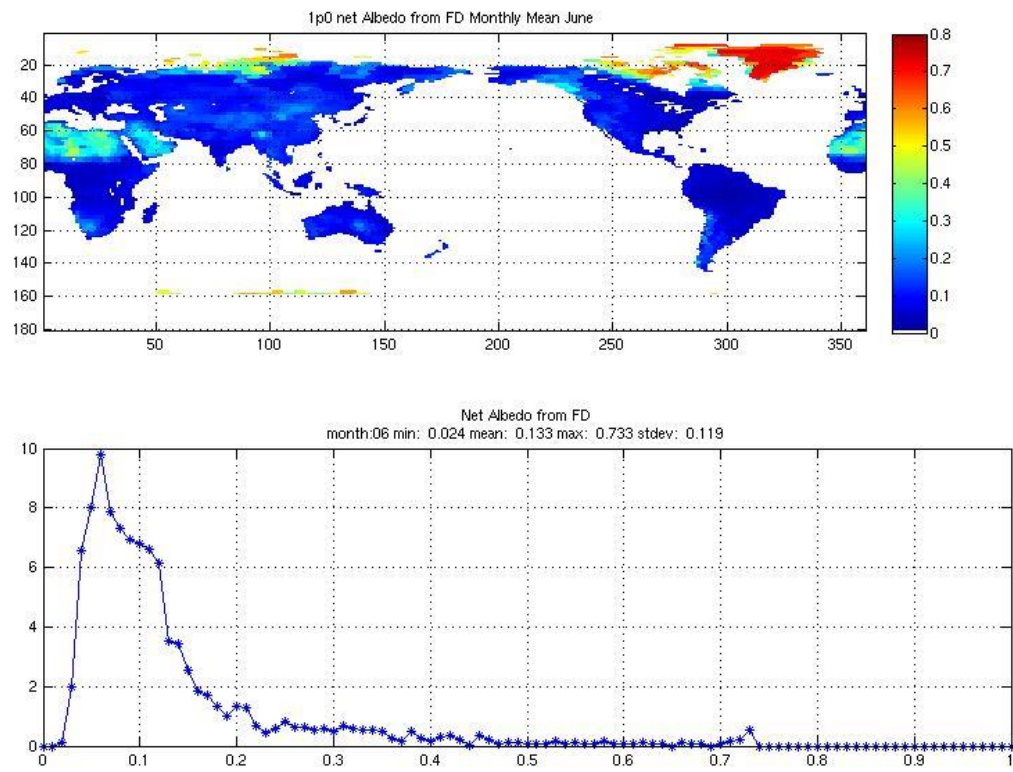


mean
MODIS bsa Albedo Map 2.13 month 06



STDEV
MODIS bsa Albedo Map 2.13 month 06





LandMet netcdf File:

